European Journal of Taxonomy 726: 102–131
https://doi.org/10.5852/ejt.2020.726.1179
ISSN 2118-9773
www.europeanjournaloftaxonomy.eu
2020 · Tumanov D.V.

Research article

urn:lsid:zoobank.org:pub:CCB2BAEF-06D4-4FAD-A018-27A54553D3DA

Integrative description of *Mesobiotus anastasiae* sp. nov. (Eutardigrada, Macrobiotoidea) and first record of *Lobohalacarus* (Chelicerata, Trombidiformes) from the Republic of South Africa

Denis V. TUMANOV [1,2]

[1] Department of Invertebrate Zoology, Faculty of Biology, Saint Petersburg State University, 199034, Universitetskaya nab. 7/9, Saint Petersburg, Russia.
[2] Marine Research Laboratory, Zoological Institute of the Russian Academy of Sciences, 199034, Universitetskaja nab. 1, Saint Petersburg, Russia.
Email: d.tumanov@spbu.ru

urn:lsid:zoobank.org:author:49E22A70-C27B-485B-941E-577666EE65F9

Abstract. A new species of the genus *Mesobiotus* is described from the Republic of South Africa using a traditional morphological approach (light and scanning electron microscopy) combined with molecular analysis (18S rRNA, 28S rRNA, ITS-2 and COI markers). *Mesobiotus anastasiae* sp. nov. differs from all known *Mesobiotus* species by having a unique combination of characters of the adult animals and the eggs. Adults of the new species have an oral cavity armature without elongate teeth in the second band, while the processes of the egg chorion have a basal collar and distinct rows of large pores. An updated key to the species of the genus *Mesobiotus*, including 66 of 70 currently described species, is given. An aquatic mite species from the *Lobohalacarus weberi* complex (freshwater Halacaridae) co-occurs with *M. anastasiae* sp. nov., suggesting that the newly described tardigrade inhabits constantly wet moss cushion habitats.

Keywords. Tardigrada, Macrobiotidae, molecular taxonomy, new species, key to species, freshwater Halacaridae, new record.

Tumanov D.V. 2020. Integrative description of *Mesobiotus anastasiae* sp. nov. (Eutardigrada, Macrobiotoidea) and first record of *Lobohalacarus* (Chelicerata, Trombidiformes) from the Republic of South Africa. *European Journal of Taxonomy* 726: 102–132. https://doi.org/10.5852/ejt.2020.726.1179

Introduction

The Tardigrada Doyère, 1840 is a phylum of microscopic multicellular animals widely distributed in nature. Currently there are more than 1300 species described (Degma *et al.* 2009–2020), but this is very likely an underrepresentation of the actual number of taxa, as the global diversity of tardigrades is poorly investigated (Bartels *et al.* 2016).

The tardigrade fauna of the Republic of South Africa is the most investigated on the African continent (Middleton 2003; McInes *et al.* 2017). However, the current state of knowledge is far from complete. Among 46 tardigrade species reported from the Republic of South Africa (McInes *et al.* 2017;

Meyer *et al.* 2018; Stec *et al.* 2020), 22 records (48%) belong to poorly described species, or members of (semi-)cryptic species complexes, whose attribution needs verification. To date, only one species of South African tardigrade (*Minibiotus ioculator* Stec, Kristensen & Michalczyk, 2020) was described using an integrative approach, including light and scanning electron microscopy investigation, as well as sequencing of molecular markers (Stec *et al.* 2020).

In 2008 I received a few moss samples collected in the Republic of South Africa. One of these samples contained a new species of the genus *Mesobiotus* Vecchi, Cesari, Bertolani, Jönsson & Guidetti, 2016. Currently this genus includes 69 species (Kaczmarek *et al.* 2020; see also Tumanov 2018b and Tumanov & Pilato 2019), being the second-largest genus in the family Macrobiotidae Thulin, 1928. A recent integrative redescription of *M. harmsworthi* (Murray, 1907), the type species of the genus (Kaczmarek *et al.* 2018), gave a powerful impetus for further research on the real diversity of *Mesobiotus*. To date, however, only a small fraction of its species have been genetically characterized, so phylogenetic relationships within the genus remains poorly resolved (Kaczmarek *et al.* 2020).

In this paper, I describe a new *Mesobiotus* species using integrative taxonomy. The detailed morphological description is supplemented by DNA sequences of four standard genes used in tardigrade taxonomy and phylogenetics (the nuclear 18S rRNA, 28S rRNA, ITS-2, and the mitochondrial COI).

An aquatic mite species of the genus *Lobohalacarus* Viets, 1939 (freshwater Halacaridae Murray, 1877), belonging to the *Lobohalacarus weberi* complex was also found in the sample, being a new record for this genus in the south African region.

Material and methods

Sampling

The moss sample was collected at the top of Table Mountain (approx. 33°57′43.9″ S, 18°24′38.0″ E, ≈1000 m a.s.l.), in the Republic of South Africa, by Irina Nikolaeva, on January 10, 2008. Material was stored within paper envelopes at room temperature. Tardigrade specimens were extracted from rehydrated samples using the standard technique of washing them through two sieves (first with ≈ 1 mm mesh size and second with 35 μm mesh size; Tumanov 2018a). The contents of the finer sieve were examined under a Leica M205C stereo microscope.

Microscopy and imaging

The tardigrades found in moss samples were fixed with acetic acid (a few drops of the concentrated acetic acid were added to the glass staining block containing tardigrade specimens in ddH_2O) and mounted on slides in Hoyer's medium. The mite specimen was directly mounted on a slide in Hoyer's medium without fixation. Light microscopy (LM): resulting permanent slides were examined under a Leica DM2500 microscope equipped with phase contrast (PhC) and differential interference contrast (DIC). Photographs were made using a Nikon DS-Fi3 digital camera with NIS software.

For scanning electron microscopy (SEM), specimens were dehydrated in an ascending ethyl alcohol series (10%, 20%, 30%, 50%, 70%, 96%) and acetone, critical-point dried in CO_2, mounted on stubs and coated with gold. A Tescan MIRA3 LMU scanning electron microscope was used for observations (Centre for Molecular and Cell Technologies, St. Petersburg State University).

Morphometrics

The sample size for morphometrics was chosen following the recommendations of Stec *et al.* (2016). Structures were measured only if their orientations were suitable. Body length was measured from the anterior end of the body to the posterior end, excluding the hind legs. The bucco-pharyngeal tube

was measured from the dorsal crests of the oral cavity armature (OCA) to the caudal end of the buccal tube, not including the buccal apophyses. Terminology for the structures within the bucco-pharyngeal apparatus and for the claws follows those of Pilato & Binda (2010) and Michalczyk & Kaczmarek (2003). Elements of the buccal apparatus, claws and eggs were measured according to Kaczmarek & Michalczyk (2017). The macroplacoid length sequence is given according to Kaczmarek *et al.* (2014). All measurements are given in micrometres (µm). The *pt* index used is the percentage ratio between the length of a structure and the length of the buccal tube (Pilato 1981), and is presented here in italics. Morphometric data were handled using ver. 1.6 of the "Parachela" template, which is available from the Tardigrada Register (Michalczyk & Kaczmarek 2013).

Genotyping

DNA was extracted from two individual animals using QuickExtract™ DNA Extraction Solution (Lucigen Corporation, USA) using the protocol kindly provided by Torbjørn Ekrem, Norwegian University of Science and Technology (see Supplementary file 1). Preserved exoskeletons were recovered, mounted on a microscope slide in Hoyer's medium and retained as the hologenophore (Pleijel *et al.* 2008).

Four genes were sequenced from one specimen: a small ribosome subunit (18S rRNA) gene, a large ribosome subunit (28S rRNA) gene, internal transcribed spacer (ITS-2), and the cytochrome oxidase subunit I (COI) gene. The primers and PCR programs used are provided in Table 1.

The PCR products were visualized in 1.5% agarose gel stained with ethidium bromide. All amplicons were sequenced directly using the ABI PRISM Big Dye Terminator Cycle Sequencing Kit (Applied Biosystems, Foster City, CA, USA) using an ABI Prism 310 Genetic Analyzer in the Core Facilities Center 'Centre for Molecular and Cell Technologies' of St. Petersburg State University. Sequences were edited and assembled using ChromasPro software (Technelysium, USA). The COI sequences were translated to amino acids using the invertebrate mitochondrial code, implemented in MEGA7 (Kumar *et al*. 2016), in order to check for the presence of stop codons and therefore of pseudogenes.

All sequences of the genus *Mesobiotus* available in GenBank at the time of the analysis were downloaded, and those originating from published works with reliable attribution of the investigated taxa were selected (see Appendix 1). Sequences of the 28S gene published by Vecchi *et al*. (2016) (KT226079–KT226087) and Guil *et al*. (2019) (MH079488, MH079489) were excluded from comparison as they do not overlap with the sequences obtained in this study. Sequences were aligned using the Muscle algorithm (Edgar 2004) with default settings, as implemented in SeaView ver. 4.0 (Gouy *et al.* 2010). Uncorrected pairwise distances were calculated using MEGA7 (Kumar *et al.* 2016) with gaps/missing data treatment set to "complete deletion". All obtained sequences were deposited in GenBank (https://www.ncbi.nlm.nih.gov/genbank/).

Mite identification

A review paper (Bartsch 1989) was used for the preliminary identification of the mite specimen found. Other publications devoted to the descriptions of *Lobohalacarus* species and subspecies, and zoogeographical records for this genus (Harvey 1988; Bartsch 1995a, 1995b, 2008, 2018), were used for the final identification.

Institutional acronyms

Specimens from the following institutions and collections were examined (curator in parentheses).

SPbU = St. Petersburg University, Russia, Faculty of Biology, Department of Invertebrate Zoology (Denis Tumanov)

UNICT = Università degli Studi di Catania, Italy, Museum of the Department of Animal Biology 'Marcello La Greca', Binda and Pilato collection (Giovanni Pilato)

Table 1. Primers and PCR programs used for amplification of the four DNA fragments sequenced in the study.

DNA fragment	Primer name	Primer direction	Primer sequence (5′–3′)	Primer source	PCR programme
COI	LCO1490	forward	GGTCAACAAATCATAAAGATATTGG	Folmer *et al.* 1994	Michalczyk *et al.* 2012
	HCO2198	reverse	TAAACTTCAGGGTGACCAAAAAATCA	Folmer *et al.* 1994	
18S rRNA	18S_Tar_Ff1	forward	AGGCGAAACCGCGAATGGCTC	Stec *et al.* 2017	Zeller (2010), *in* Stec *et al.* 2015
	18S_Tar_Rr1	reverse	GCCGCAGGCTCCACTCCTGG	Stec *et al.* 2017	
	18Sfw	forward	CTTGTCTCAAAGATTAAGCCATGCA	Dabert *et al.* 2010	
28S rRNA	28S_Eutar_F	forward	ACCCGCTGAACTTAAGCATAT	Gąsiorek *et al.* 2018	Mironov *et al.* 2012
	28S_R0990	reverse	CCTTGGTCCGTGTTTCAAGAC	Mironov *et al.* 2012	
ITS-2	ITS2_Eutar_Ff	forward	CGTAACGTGAATTGCAGGAC	Stec *et al.* 2018a	Stec *et al.* 2018a
	ITS2_Eutar_Rr	reverse	TGATATGCTTAAGTTCAGCGG	Stec *et al.* 2018a	

Results

Phylum Tardigrada Doyère, 1840
Class Eutardigrada Richters, 1926
Superfamily Macrobiotoidea Thulin, 1928
Family Macrobiotidae Thulin, 1928
Genus *Mesobiotus* Vecchi, Cesari, Bertolani, Jönsson, Rebecchi & Guidetti, 2016

Mesobiotus anastasiae sp. nov.
urn:lsid:zoobank.org:act:8651D164-4CBC-41DD-A5C4-FF9E584F8088
Figs 1–6, Tables 2–3

Etymology

I dedicate this new species to my daughter, Anastasia.

Material examined

Holotype

REPUBLIC OF SOUTH AFRICA • ♀; Cape Town, top of Table Mountain; approx. 33°57′43.9″ S, 18°24′38.0″ E; ≈1000 m a.s.l.; 10 Jan. 2008; I. Nikolaeva leg.; moss on soil, wet depression with a small temporary pond; SPbU 256(8).

Paratypes

REPUBLIC OF SOUTH AFRICA • 5 ♀♀, 3 ♂♂, 22 eggs; same collection data as for holotype; SPbU 256(1) to 256(6) and 256(9) to 256(18) • 2 adults, 7 eggs; same collection data as for holotype; SEM stub; SPbU_Tar16.

Comparative material

PEOPLE'S REPUBLIC OF CHINA • 7 eggs, paratypes of *Mesobiotus mauccii* (Pilato, 1974); Canton; moss on tree bark; UNICT 2132.

Morphological description

Body elongated (Fig. 1A–B) (morphometrics in Table 2, raw morphometric data are provided in Supplementary file 2). Fresh specimens uncolored or whitish with slightly greenish gut content,

transparent after fixation in Hoyer's medium. Four specimens with eyes (Fig. 1A), usually well-discernible after slide mounting, three specimens without eyes; in two specimens processed for DNA extraction the presence or absence of eyes was not registered. Dorsal cuticle in LM with poorly visible network-like pattern (Fig. 2A). SEM investigation revealed presence of flat tubercles all over the body surface (Fig. 2B–C). Additionally, the body surface is covered with regularly distributed small granules (invisible in LM; Fig. 2B). In the dorso-lateral position, above the bases of the hind legs, zones of concentrated granules are present (Fig. 2C). All legs with granulated areas. Legs I–III with small granulated areas on the external surfaces, near the claw bases (Fig. 4A), invisible or extremely poorly visible in LM (Fig. 4D, black arrowhead), the internal leg surfaces without granulation, with indistinct pulvinus (Fig. 4B, white asterisk). Legs IV with better-developed granulation dorsally (Fig. 2D) and around the claw bases (Fig. 4G).

Buccal-pharyngeal apparatus of *Macrobiotus* type (Fig. 3A) with ventral lamina and ten peribuccal lamellae. Oral cavity armature (OCA) of modified *krynauwi* type (according to Kaczmarek *et al*. 2020) with three bands of teeth visible in LM. Evident first (anterior) band consists of a single uneven line of relatively large and slightly longitudinally elongated teeth (Fig. 3F, J–K, O, black arrowheads). Second band consists of a wide zone of small dot-like teeth (Fig. 3G, I, L, N), teeth of the anterior-most and

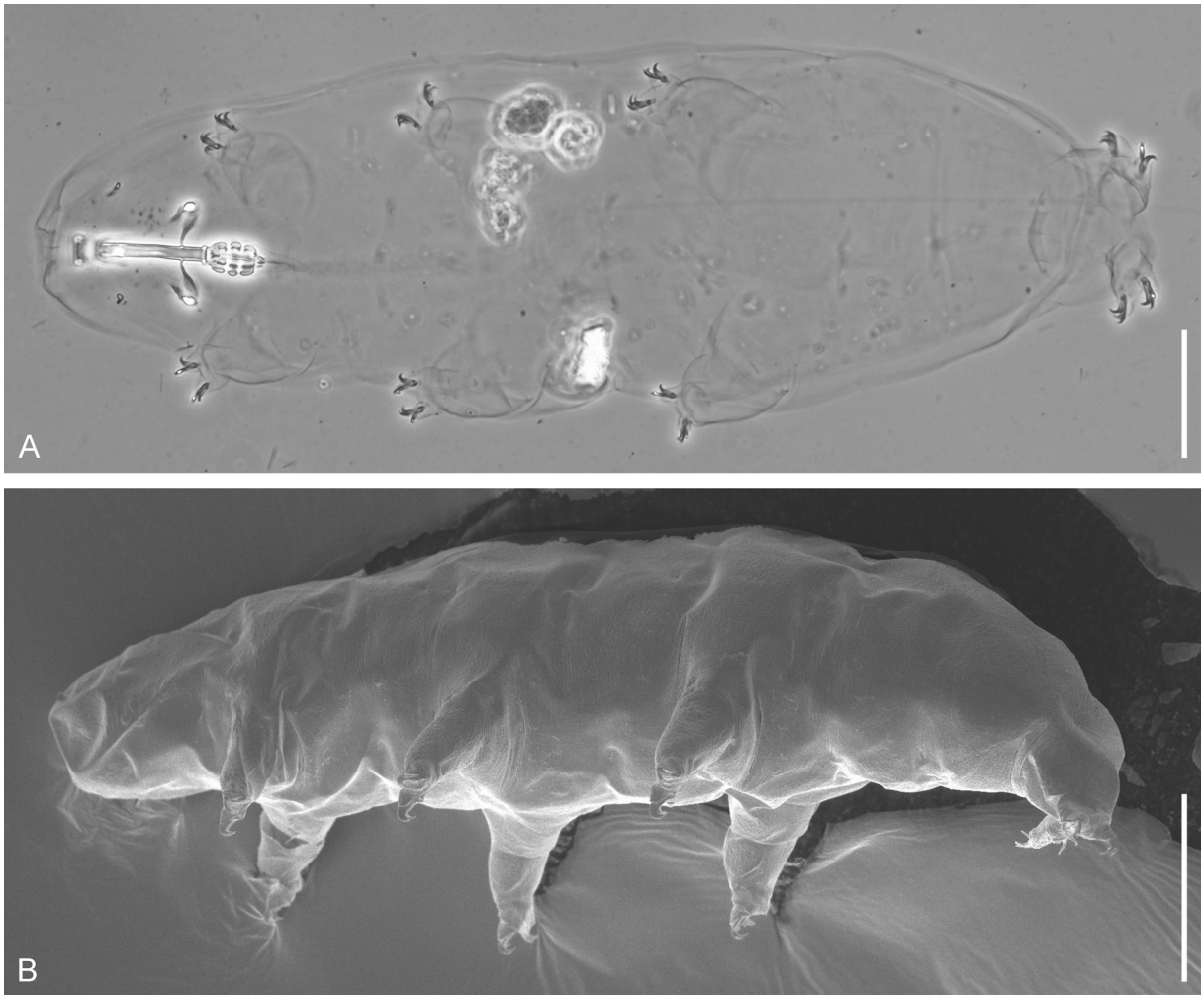

Fig. 1. *Mesobiotus anastasiae* sp. nov., total view. **A**. Holotype, ♀ (SPbU 256(8)). Dorso-ventral view, PhC. **B**. Paratype (SPbU_Tar16). Lateral view in SEM. Scale bars = 50 µm.

Table 2. Summary of morphometric data for *Mesobiotus anastasiae* sp. nov. Measurements are given in µm, *pt* values in % (the *pt* index is the percentage ratio between the length of a structure and the length of the buccal tube).

CHARACTER	N	RANGE		MEAN		SD		Holotype	
		µm	*pt*	µm	*pt*	µm	*pt*	µm	*pt*
Body length	7	284–426	*809–1002*	366	*909*	44	*83*	426	*1002*
Buccopharyngeal tube									
Buccal tube length	9	35.1–45.5	–	40.8	–	3.5	–	42.6	–
Stylet support insertion point	9	26.5–35.8	*75.3–78.7*	31.5	*77.1*	3.1	*1.2*	33.1	*77.8*
Buccal tube external width	7	4.1–6.0	*11.3–13.1*	5.1	*12.2*	0.6	*0.6*	5.4	*12.7*
Buccal tube internal width	7	2.8–4.0	*7.6–8.8*	3.4	*8.2*	0.4	*0.4*	3.6	*8.5*
Ventral lamina length	9	21.9–30.7	*62.2–67.4*	26.2	*64.1*	2.7	*1.7*	27.1	*63.8*
Placoid lengths									
Macroplacoid 1	9	3.7–6.1	*10.0–13.4*	4.8	*11.7*	0.9	*1.3*	5.2	*12.2*
Macroplacoid 2	9	2.8–4.4	*8.0–10.3*	3.6	*8.9*	0.5	*0.7*	4.4	*10.3*
Macroplacoid 3	9	3.2–6.4	*9.1–14.6*	4.7	*11.4*	1.1	*1.9*	5.4	*12.6*
Microplacoid	9	2.0–3.3	*5.3–7.7*	2.6	*6.3*	0.5	*0.9*	3.3	*7.7*
Macroplacoid row	9	11.7–18.3	*33.0–41.9*	15.1	*36.8*	2.5	*3.2*	16.6	*38.9*
Placoid row	9	13.9–21.5	*39.0–49.0*	18.2	*44.3*	2.9	*3.9*	19.7	*46.2*
Claw 1 lengths									
External primary branch	5	7.6–10.8	*21.6–24.5*	9.4	*23.1*	1.2	*1.2*	9.9	*23.4*
External secondary branch	5	5.9–8.0	*16.8–19.1*	7.2	*17.7*	0.8	*0.9*	7.4	*17.5*
Internal primary branch	7	7.3–10.5	*20.8–23.8*	9.0	*22.2*	1.0	*1.0*	9.4	*22.0*
Internal secondary branch	7	5.9–8.3	*16.1–18.2*	7.0	*17.3*	0.8	*0.9*	6.8	*16.1*
Claw 2 lengths									
External primary branch	6	8.0–10.8	*22.4–24.7*	9.4	*23.5*	1.0	*0.9*	10.2	*23.9*
External secondary branch	6	6.6–8.4	*17.2–19.3*	7.4	*18.5*	0.7	*0.7*	8.0	*18.9*
Internal primary branch	6	7.4–10.1	*21.0–23.8*	9.0	*22.6*	1.1	*1.1*	10.1	*23.8*
Internal secondary branch	6	6.0–7.7	*16.2–19.4*	7.0	*17.5*	0.6	*1.1*	7.7	*18.1*
Claw 3 lengths									
External primary branch	6	7.8–10.9	*22.0–25.1*	9.5	*23.5*	1.1	*1.3*	10.3	*24.1*
External secondary branch	6	6.1–8.8	*17.2–20.1*	7.5	*18.4*	0.9	*1.1*	8.0	*18.7*
Internal primary branch	7	7.1–10.7	*20.2–24.6*	9.4	*22.8*	1.3	*1.4*	10.1	*23.8*
Internal secondary branch	7	5.8–8.2	*16.4–18.4*	7.2	*17.4*	0.9	*0.9*	7.8	*18.4*
Claw 4 lengths									
Anterior primary branch	6	9.8–12.3	*24.7–28.2*	11.1	*26.4*	1.0	*1.2*	11.4	*26.9*
Anterior secondary branch	6	7.0–8.6	*17.0–20.3*	7.9	*18.8*	0.6	*1.1*	8.6	*20.3*
Posterior primary branch	5	11.7–12.9	*27.2–30.2*	12.3	*28.6*	0.6	*1.2*	12.9	*30.2*
Posterior secondary branch	5	8.0–9.4	*18.7–20.6*	8.6	*19.9*	0.6	*0.7*	8.7	*20.4*

(rarely) posterior-most rows of the second band are slightly larger than others, sometimes teeth of the anterior-most row are very slightly longitudinally elongated. Third band comprises three dorsal and three ventral transverse ridges (Fig. 3H, J, M, O). Medio-ventral ridge is usually more or less clearly divided into two separate parts (Fig. 3J, O). Pharyngeal bulb with apophyses, three macroplacoids and a large microplacoid (Fig. 3A). Macroplacoid length sequence is 2 < 3 = 1. First macroplacoid is anteriorly

narrowed, third macroplacoid without distinct subterminal constriction, but with strong terminal protrusion, directed towards pharynx lumen (Fig. 3B–E, black arrowheads).

Claws of *Mesobiotus* type with minute stalk, distinct distal part of the basal portion, short common tract and developed internal septum, defining a distal part. Primary and secondary branches diverge at a point near half the claw height, main branches with long accessory points, which at a large distance from the main claw (Fig. 4C, E–F, H). Claws of fourth pair of legs slightly longer than claws of first three pairs of legs (Fig. 4H). All claws with smooth lunules (Fig. 4C, E–F, H). Anterior (internal) and posterior (external) claws of legs IV are similar in shape, with equally sized lunules. Poorly developed bar-like cuticular thickenings are present below claw bases of the first three pairs of legs (Fig. 4C, black arrowhead). Claws of legs IV are connected with a wide horseshoe-like structure (Fig. 4F, black arrowhead).

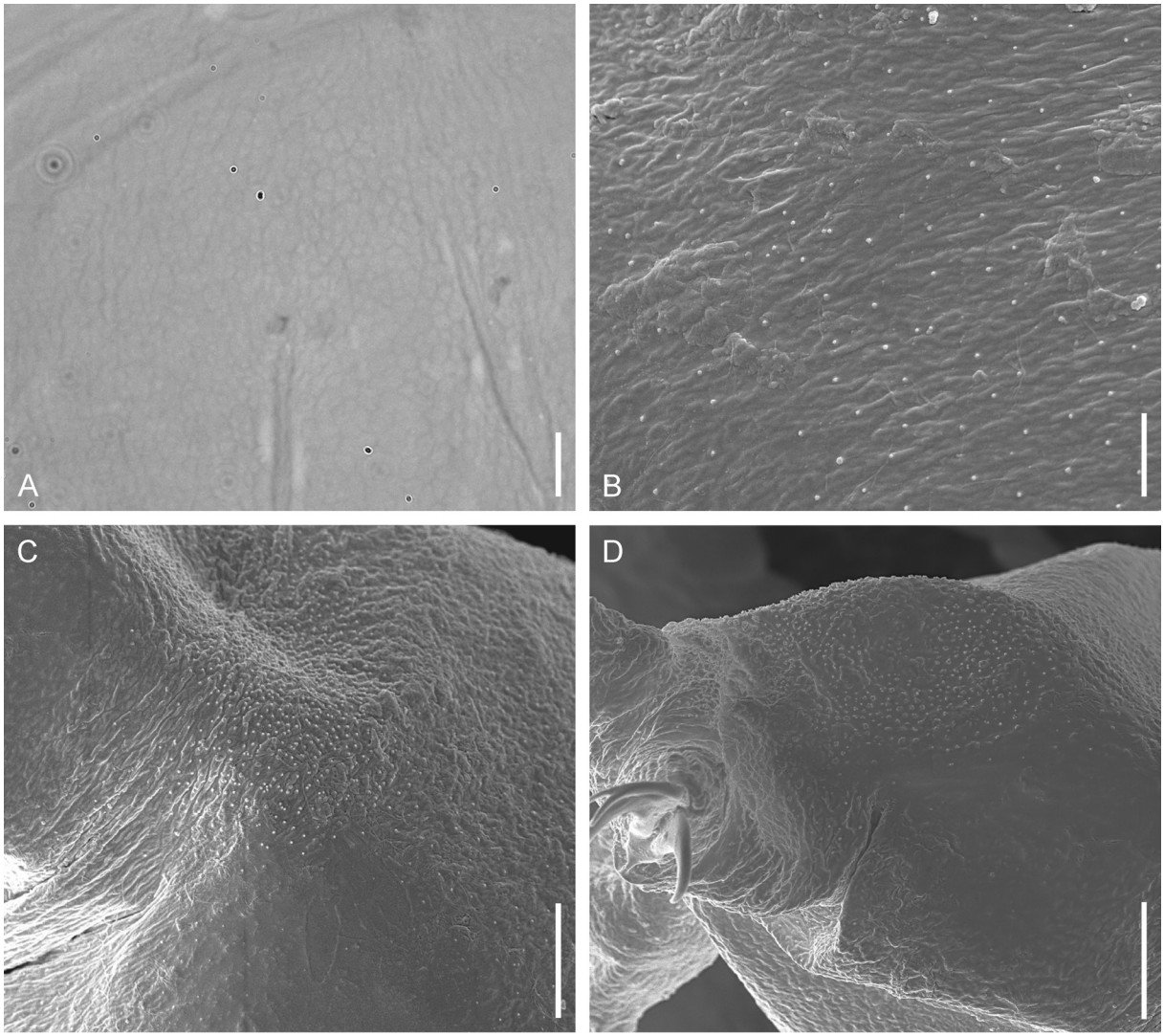

Fig. 2. *Mesobiotus anastasiae* sp. nov., cuticular sculpture. **A**. Paratype (SPbU 256(18)). Sculpture of the dorsal body surface, PhC. **B–D**. Paratype (SPbU_Tar16). **B**. High magnification of the sculpture of the dorsal body surface, SEM. **C**. Dorso-lateral zone of concentrated cuticular dots, SEM. **D**. Dot-like sculpture on the dorsal side of hind legs, SEM. Scale bars A, C, D = 5 μm; B = 2 μm.

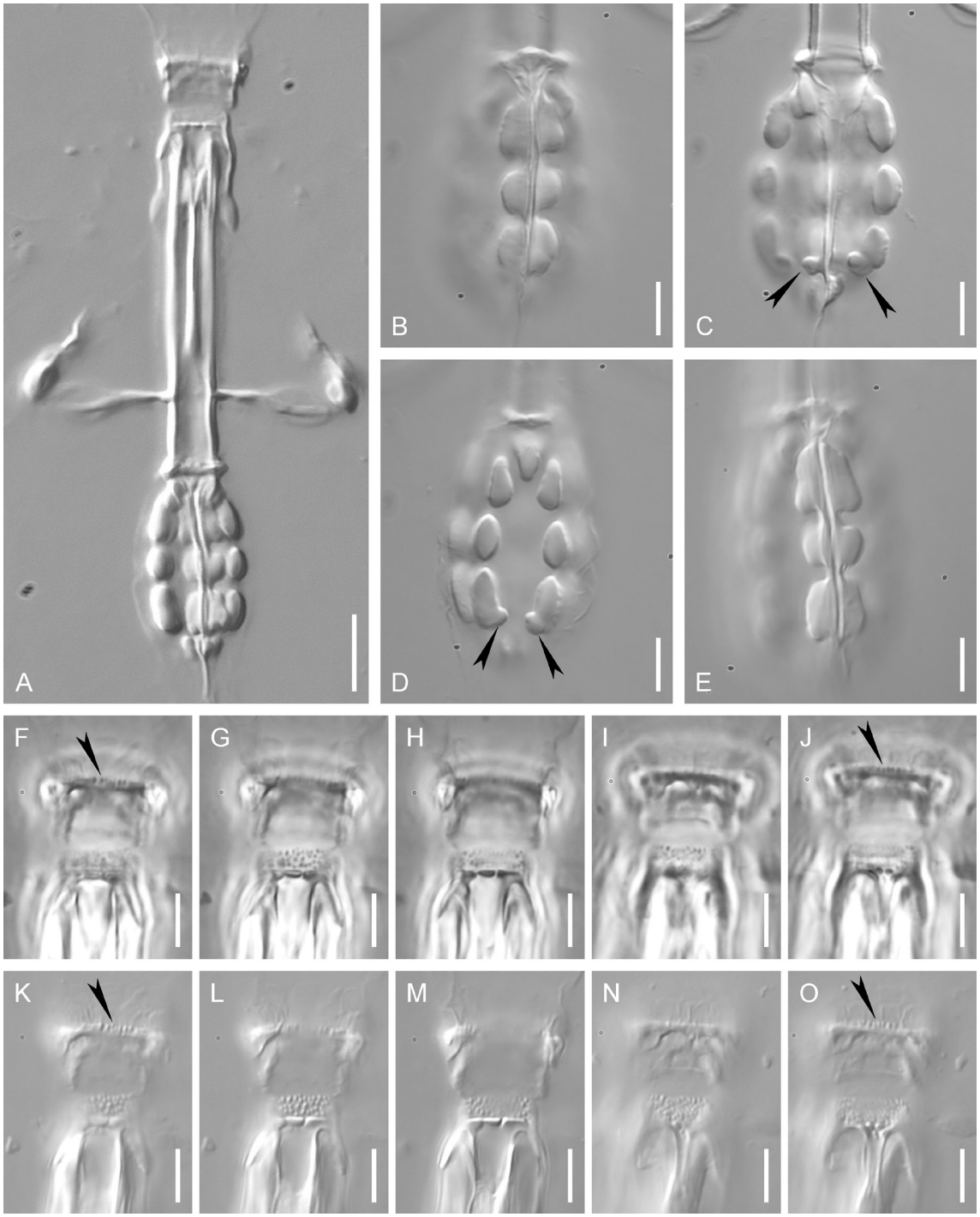

Fig. 3. *Mesobiotus anastasiae* sp. nov., bucco-pharyngeal apparatus. **A, E–O**. Paratype, ♀ (SPbU 256(9)). **B–D**. Holotype, ♀ (SPbU 256(8)). **A**. Total dorso-ventral view of the bucco-pharyngeal apparatus, DIC. **B**. Ventral row of macroplacoids, focused on their outer surface, DIC. **C**. Ventral row of macroplacoids, focal plane shifted deeper into the parynx, black arrowheads indicate appendices of the third macroplacoid bent inward, DIC. **D**. Lateral rows of macroplacoids, black arrowheads indicate appendices of the third macroplacoid bent inward, DIC. **E**. Ventral row of macroplacoids, focused on their outer surface; note the absence of the preterminal constriction of the third macroplacoid, DIC. **F–O**. Oral cavity armature, dorsal (F–H, K–M) and ventral view (I–J, N–O), black arrowheads indicate teeth of the first band, F–J = PhC, K–O = DIC. Scale bars: A = 10 μm; B–O = 5 μm.

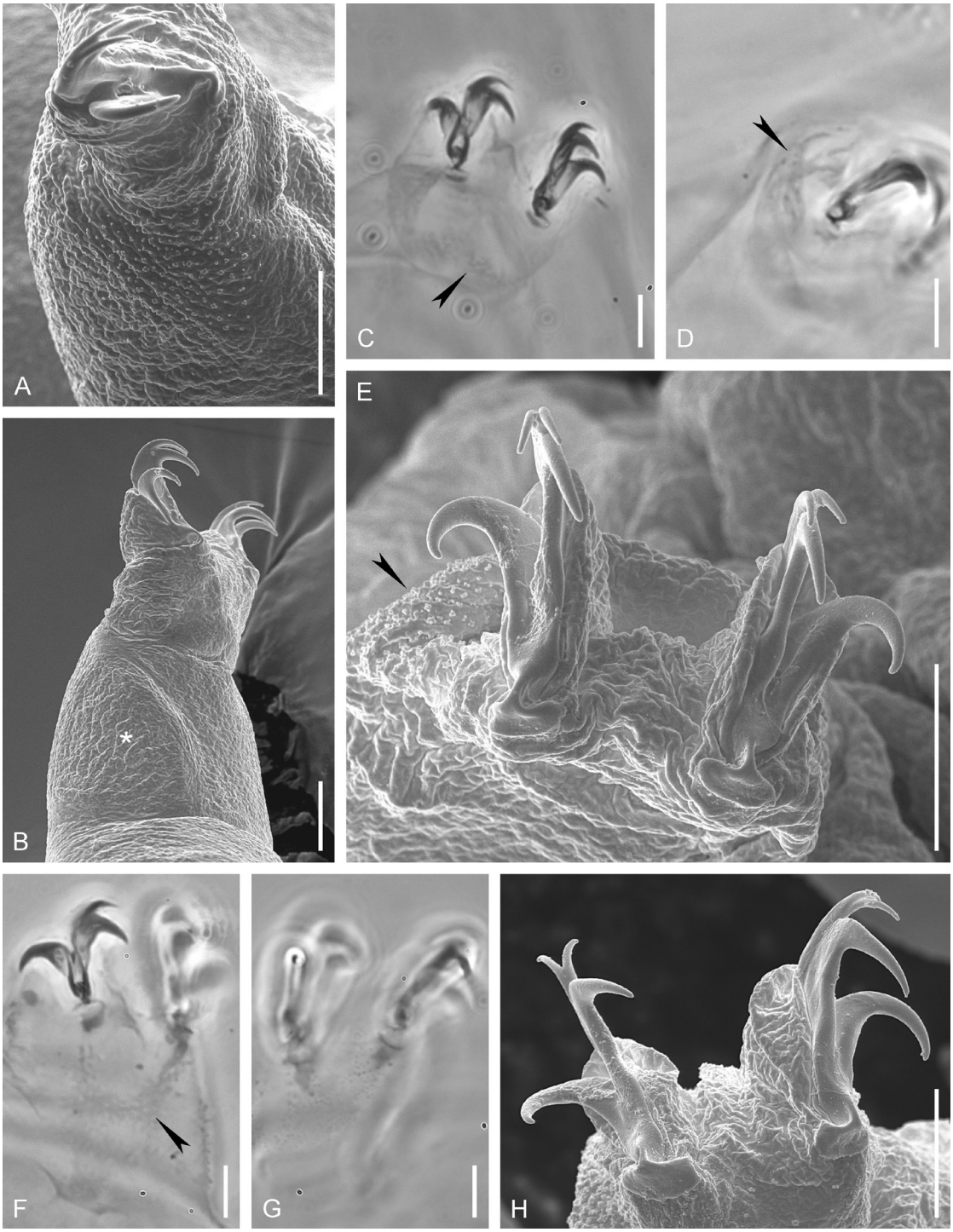

Fig. 4. *Mesobiotus anastasiae* sp. nov., paratype (SPbU_Tar16). Legs. **A**. External surface of leg III with developed dot-like sculpture, SEM. **B**. Internal surface of leg II without dot-like sculpture, white asterisk – pulvinus on the inner side of the leg, SEM. **C**. Claws of leg I, black arrowhead indicates bar-like cuticular thickening (holotype), PhC. **D**. Leg II, black arrowhead indicates dot-like sculpture on the external surface (SPbU 256(1), paratype), PhC. **E**. Claws of leg II, black arrowhead indicates dot-like sculpture on the external surface of the leg, SEM. **F**. Claws of leg IV, black arrowhead indicates horseshoe-like structure (SPbU 256(13), paratype), PhC. **G**. Leg IV, dot-like sculpture on the ventral surface (holotype), PhC. **H**. Claws of leg IV, SEM. Scale bars = 5 μm.

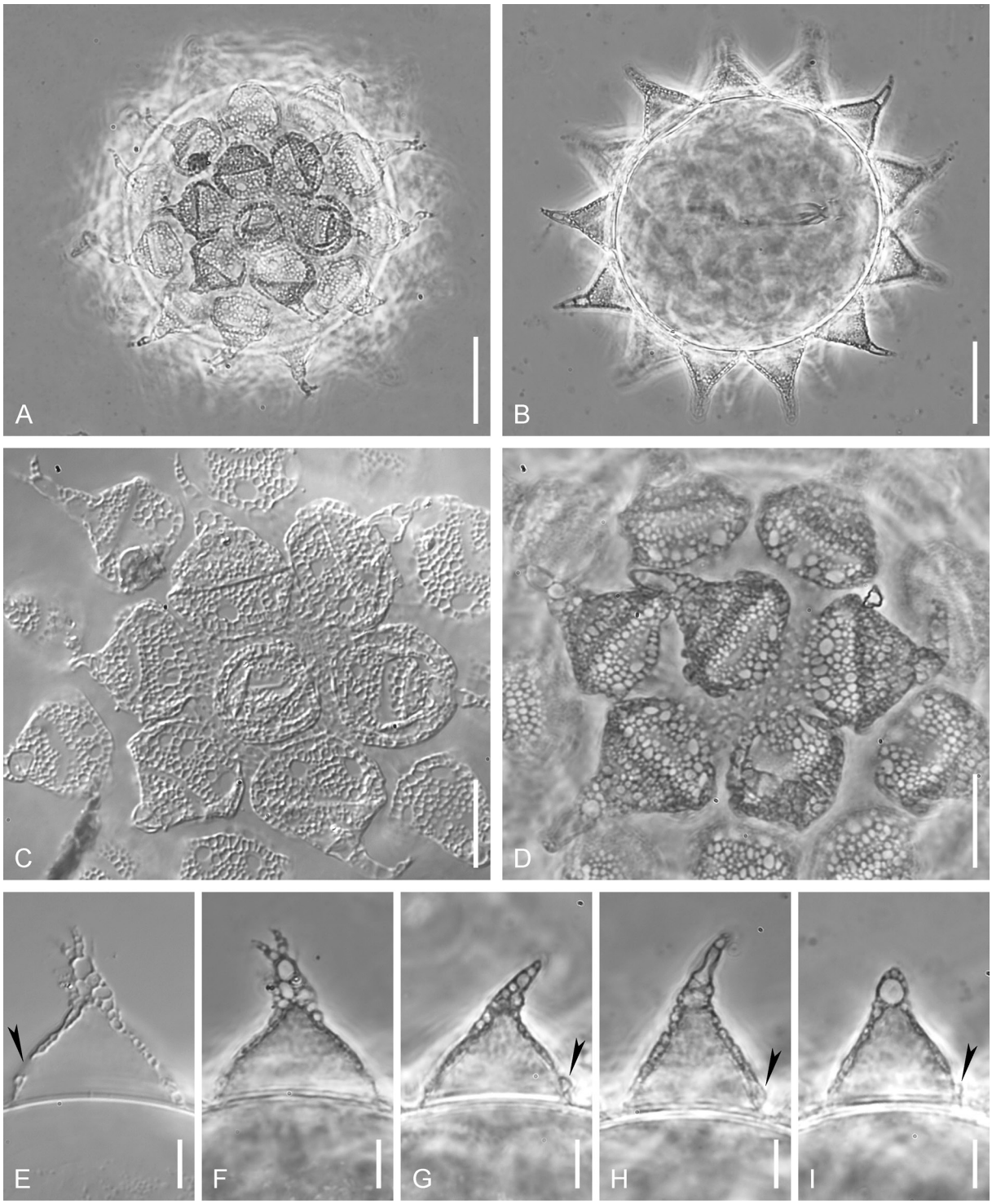

Fig. 5. *Mesobiotus anastasiae* sp. nov., eggs. **A–F**. Paratype (SPbU 256(15)). **G–I**. Paratype (SPbU 256(4)). **A**. Total view of the egg surface, PhC. **B**. Total view of the optical section of the embryonated egg, PhC. **C–D**. Details of the egg surface, DIC, PhC. **E**. Optical section of the egg process, black arrowhead indicates pore, DIC. **F–I**. Optical sections of different egg processes, black arrowheads indicate collar, PhC. Scale bars: A–B = 20 μm; C–D = 10 μm; E–I = 5 μm.

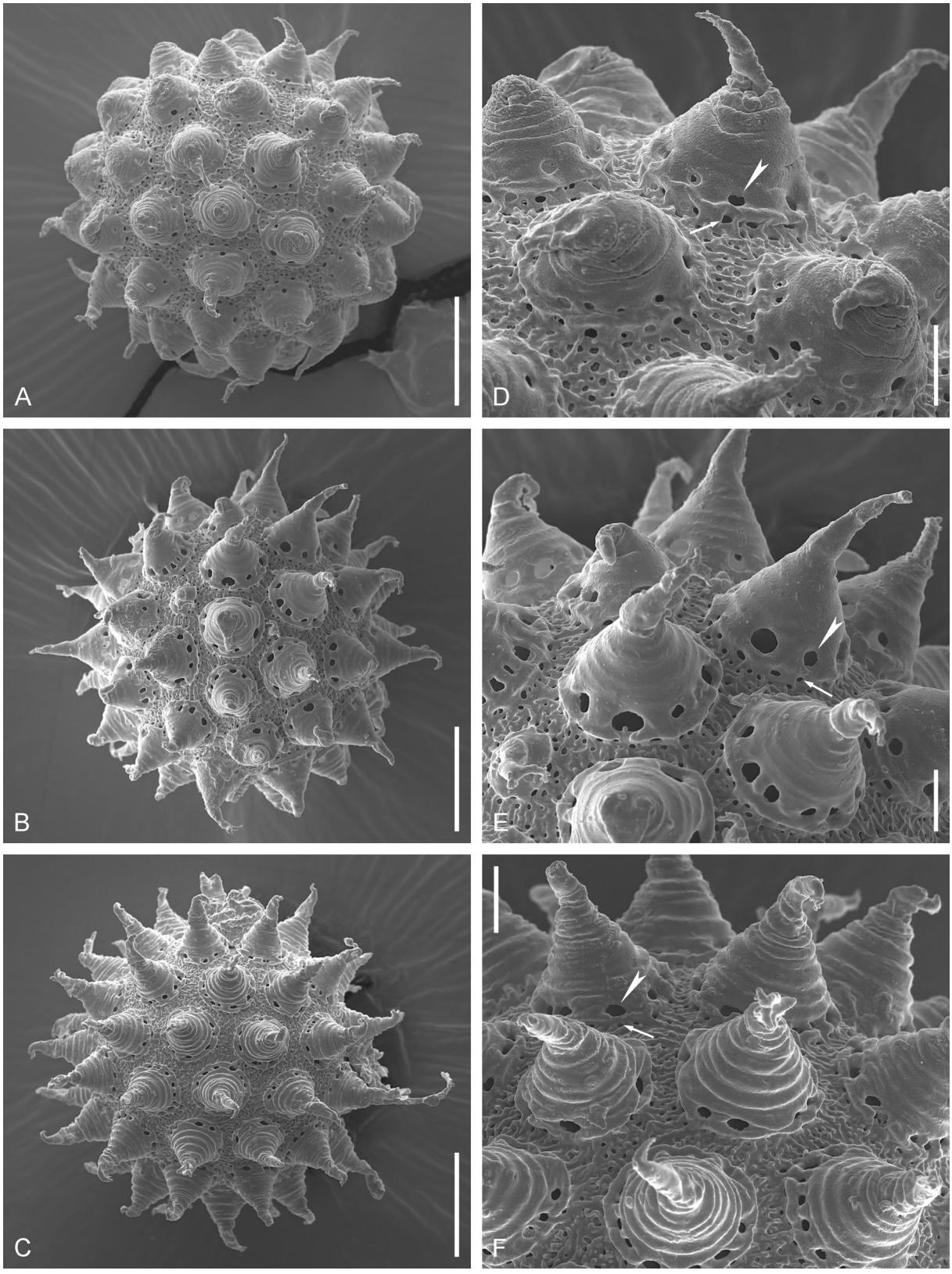

Fig. 6. *Mesobiotus anastasiae* sp. nov., paratype (SPbU_Tar16). Eggs. **A–C**. Total view of the egg, SEM. **D–F**. Details of the egg surface, white arrowheads indicate pores above the collar, white arrows indicate pores below the collar, SEM. Scale bars: A–C = 20 μm; D–F = 5 μm.

Table 3. Measurements (in μm) of selected morphological structures of eggs of *Mesobiotus anastasiae* sp. nov. Abbreviations: N = number of eggs/structures measured, range refers to the smallest and the largest structure among all measured specimens; SD = standard deviation.

CHARACTER	N	RANGE	MEAN	SD
Egg bare diameter	13	61.7–74.7	66.7	4.0
Egg full diameter	13	84.6–108.5	95.9	7.1
Process height	39	14.6–21.3	17.7	1.8
Process base width	39	11.8–18.6	15.5	1.6
Process base/height ratio	39	63%–117%	88%	9%
Inter-process distance	39	0.0–3.8	1.3	0.9
Number of processes on egg circumference	13	12–15	13.4	0.9

Eggs spherical, white, ornamented and laid freely (Figs 5A–B, 6A–C; morphometrics in Table 3). Chorion with conical processes that can be attributed to the "*sharp wide cones with collars*" and "*reticular design with "bubbles"*" morphotypes (according to Kaczmarek *et al*. 2020). Egg processes with wide bases and thinned and flexible apices (Figs 5C–I, 6D–F). Basal parts of the processes with bilayered walls, with a net of trabecular structures between the internal and external layers, forming irregular rounded meshes of different size, so the processes seem to be reticulated in LM (Fig. 6C–I). Apical parts of the processes with bubble-like internal structure (Fig. 5E–I), often branching (Figs 5E–F, 6E–F). The SEM observations revealed circular wrinkles on the outer surface of the processes (Fig. 6D–F). Basal parts of the processes with well-developed collar elevated above the egg surface (Figs 5G–I, black arrowheads; 6D–F). Large pores (1–3 μm in diameter), visible in LM and in SEM, are present on the surface of all processes, near the collar, in two rows: one row of larger pores above the collar and second row of smaller pores below the collar (Figs 5C–E, black arrowhead; 6D–F). Process bases are smooth, without a crown of granules or teeth. Egg surface between the processes without areolation, with a system of

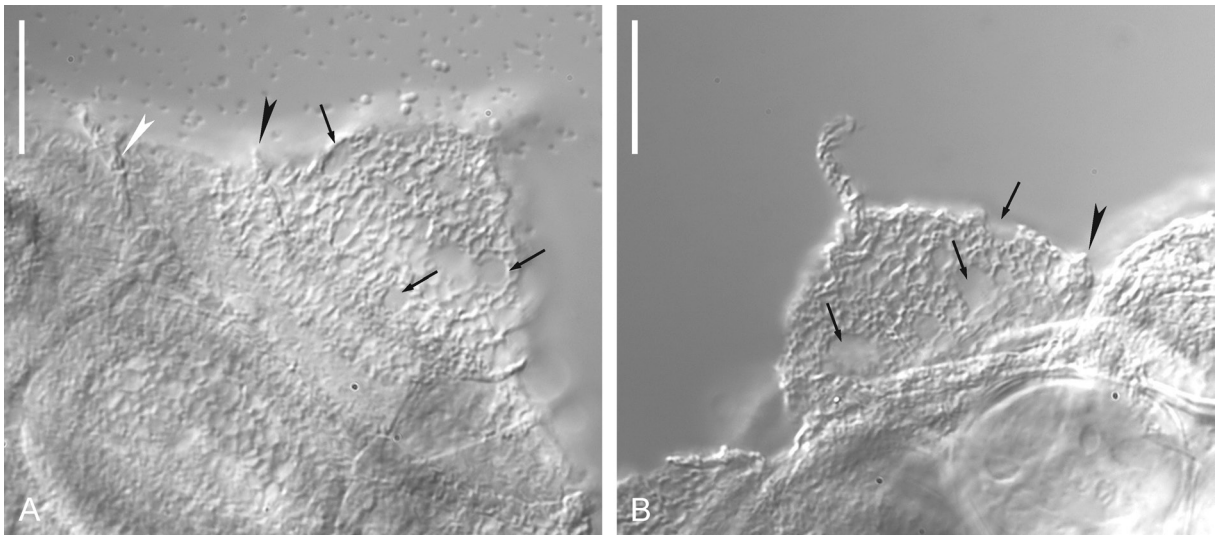

Fig, 7. *Mesobiotus mauccii* (Pilato, 1974). Paratype egg (UNICT 2132). **A–B**. Egg processes, white arrowhead indicates polygonate mesh-like pattern, black arrowheads indicate the collar, black arrows indicate pores, DIC. Scale bars: 10 μm.

irregularly distributed ridges and small pores between them (Fig. 6D–F). In some eggs underdeveloped small processes are present among normal processes (Fig. 6B, E).

Reproduction

The new species is dioecious. Adult males were identified by having testis filled with spermatozoa, visible under PhC on mounted slides. Males of *M. anastasiae* sp. nov. exhibit no secondary sexual dimorphism.

DNA sequences

Sequences of good quality for the four aforementioned molecular markers were obtained from one specimen (voucher slide SpbU 256(11)):

COI sequence (GenBank: MT904513), 658 bp long;
18S rRNA sequence (GenBank: MT903468), 1030 bp long;
28S rRNA sequence (GenBank: MT903612), 740 bp long;
ITS-2 sequence (GenBank: MT903470), 419 bp long.

Phylum Arthropoda von Siebold, 1848
Subphylum Chelicerata Heymons, 1901
Class Arachnida Lamarck, 1801
Superorder Acariformes Zakhvatkin, 1952
Family Halacaridae Murray, 1877

Lobohalacarus cf. ***weberi*** (Romijn & Viets, 1924)
Fig. 8

Material examined

REPUBLIC OF SOUTH AFRICA • 1 ♀; Cape Town, top of Table Mountain; approx. 33°57′43.9″ S, 18°24′38.0″ E; ≈ 1000 m a.s.l.; 10 Jan. 2008; I. Nikolaeva leg.; moss on soil, wet depression with a small temporary pond; SPbU 256(20).

During sample processing, a single mite specimen from the family Halacaridae (Chelicerata, Trombidiformes) was found (Fig. 8A). In having an undivided ventral shield (Fig. 8B) and developed frontal spine (Fig. 8C) this specimen undoubtedly belongs to the *Lobohalacarus weberi* complex of species, and is the first record of this genus from southern Africa (Bartsch 2018). Apart from its nominative variable species *Lobohalacarus weberi* (Romijn & Viets, 1924), this complex includes several similar species and subspecies with unclear taxonomic status (Bartsch 1995a, 2018). The studied specimen is similar to *Lobohalacarus weberi tristanensis* Bartsch, 1995 (known from Tristan da Cunha Islands only) by having genu I with two ventral spines (Fig. 8A, black arrows) and genital sclerites with two pairs of genital acetabula (Fig. 8D, white arrowheads), but differs from this form by having five pairs of perigenital setae (Fig. 8B, white arrowheads).

Discussion

Phenotypic differential diagnosis of *Mesobiotus anastasiae* sp. nov.

Adult animals

Within the genus *Mesobiotus*, only two species have OCA of the *krynauwi* type – without the row of the longitudinally elongated teeth in the second band and with a developed first row of teeth: *M. krynauwi* (Dastych & Harris, 1995) and *M. tehuelchensis* (Rossi, Claps & Ardohain, 2009).

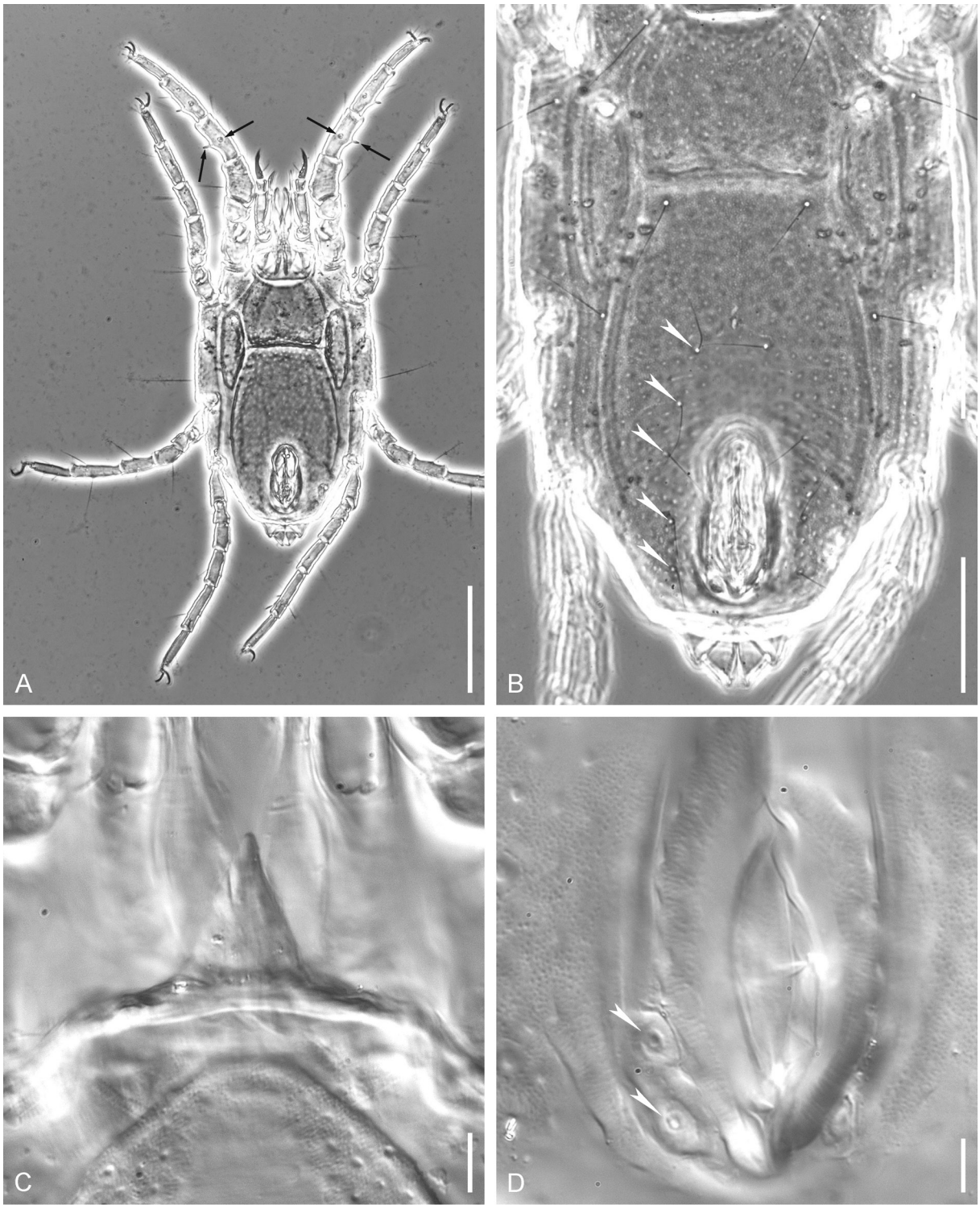

Fig. 8. *Lobohalacarus* cf. *weberi*, ♀ (SPbU 256(20)). **A**. Total view, black arrows indicate spines on genua I, PhC. **B**. Ventral shield, white arrowheads indicate bases of perigenital setae, PhC. **C**. Frontal spine, DIC. **D**. Genital opening, white arrowheads indicate genital acetabula, DIC. Scale bars: A = 100 μm; B = 50 μm; C = 10 μm; D = 5 μm.

Mesobiotus anastasiae sp. nov. differs from *M. krynauwi* (Dastych & Harris, 1995) (known from several locations in Antarctica only, Dastych & Harris 1995) by having cuticle with thin reticulate pattern visible in PhC (smooth cuticle with small pores in *M. krynauwi*), by having the first band of teeth of OCA consisting of a single line of elongated teeth (several lines of minute dot-like teeth in *M. krynauwi*), by having lunules of the hind legs without teeth (usually with sharp teeth in *M. krynauwi*), by having eggs with a smaller bare egg diameter (61.7–74.7 µm in *M. anastasiae* sp. nov. vs 98–115 µm in *M. krynauwi*), larger egg processes (processes height 14.6–21.3 µm in *M. anastasiae* sp. nov. vs 9–14 µm in *M. krynauwi*) with large pores and collar (absent in *M. krynauwi*), and by having the egg surface between processes with ridges and pores (smooth in *M. krynauwi*).

Mesobiotus anastasiae sp. nov. differs from *M. tehuelchensis* (Rossi, Claps & Ardohain, 2009) (known only from the type locality in Agentina, Rossi *et al*. 2009) by having cuticle with thin reticulate pattern visible in PhC (smooth cuticle in *M. tehuelchensis*), by having the first band of teeth of OCA consisting of a single line of elongated teeth (several lines of minute dot-like teeth in *M. tehuelchensis*), by having a thinner buccal tube (external buccal tube width is 4.1–6.0 µm vs 9.9–14.9 µm in *M. tehuelchensis*), by having eggs with a smaller bare egg diameter (61.7–74.7 µm in *M. anastasiae* sp. nov. vs 77 µm in *M. tehuelchensis*), and smaller egg processes (processes height 14.6–21.3 µm in *M. anastasiae* sp. nov. vs ≈50 µm in *M. tehuelchensis*) with large pores and a collar (absent in *M. tehuelchensis*).

Eggs

Based on the morphology of the processes, eggs of *M. anastasiae* sp. nov. should be attributed to the "*sharp wide cones with collar*" morphotype (Kaczmarek *et al.* 2020). Within the genus *Mesobiotus* only two species have this type of egg processes: *M. joenssoni* Guidetti *et al*., 2019 and *M. mauccii* (Pilato, 1974) (the former species' eggs were erroneously attributed to the "*sharp narrow cones*" morphotype in Kaczmarek *et al*. (2020)). In all three species, the conical processes have a wide base with a developed collar (or "*circular thickness*" (Guidetti *et al.* 2019)), situated on the process wall above the egg surface. Additionally, the egg processes of all three species bear large pores on their side walls.

Mesobiotus anastasiae sp. nov. differs from *M. joenssoni* (known only from the type locality on Elba Island, Italy, Guidetti *et al.* 2019) by having cuticle with thin reticulate pattern visible in PhC (cuticle with large (visible in LM) granules in the caudal region of the dorsal side in *M. joenssoni*), by having OCA without elongated teeth in the second band (developed in *M. joenssoni*), by having the first band of teeth of OCA consisting of a single line of elongated teeth (several lines of minute dot-like teeth in *M. joenssoni*), by having eggs with smaller egg processes (processes height 14.6–21.3 µm in *M. anastasiae* sp. nov. vs 27–36 µm in *M. joenssoni*) with larger and more numerous pores above the collar, and with a second line of pores below the collar (absent in *M. joenssoni*).

Mesobiotus anastasiae sp. nov. differs from *M. mauccii* (known from several Asian locations: China (Pilato 1974; Beasley & Miller 2007, 2012), South Andaman Island (Maucci & Durante Pasa 1980), Japan (Utsugi 1988; Abe & Takeda 2000, 2005)) by having cuticle with thin reticulate pattern visible in PhC (cuticle smooth in *M. mauccii*), by having OCA without elongated teeth in the second band (developed in *M. mauccii*), by having the first band of teeth of OCA consisting of a single line of elongated teeth (several lines of minute dot-like teeth in *M. mauccii*), by having a thinner buccal tube (external buccal tube width is 4.1–6.0 µm vs ca 11 µm in *M. mauccii* type material), by having egg processes with numerous pores arranged in lines above and below the collar (rare single pores are distributed all over the process surface in *M. mauccii*), and in lacking ridges on the egg surface between the processes, forming a mesh-like pattern with polygonate cells circling each process (Fig. 7A–B).

Genotypic differential diagnosis of *Mesobiotus anastasiae* sp. nov.

The ranges of uncorrected genetic *p*-distances between the studied population of *Mesobiotus anastasiae* sp. nov. and other species of the genus *Mesobiotus,* for which sequences are available from GenBank (see Appendix 1), are as follows:

COI: 19.15%–26.60% (mean 21.66%), with the most similar being *M.* gr. *furciger* from Norway (MH195153, Kaczmarek *et al.* 2018), and the least similar being *M. furciger* (Murray, 1907) from Antarctica (JX865308, Czechowski *et al.* 2012).

18S rRNA: 1.29%–6.01% (mean 3.47%), with the most similar being *M. occultatus* Kaczmarek, Zawierucha, Buda, Stec, Gawlak, Michalczyk & Roszkowska, 2018 from Svalbard (MH197147, Kaczmarek *et al.* 2018), and the least similar being *M. dilimanensis* from the Philippines (MN257048, Itang *et al*. 2020).

28S rRNA: 4.56%–12.11% (mean 7.70%), with the most similar being *M. harmsworthi* (Murray, 1907) from Svalbard (MH197264, Kaczmarek *et al.* 2018), and the least similar being *M. dilimanensis* (MN257049, Itang *et al*. 2020).

ITS-2: 13.03%–29.83% (mean 20.47%), with the most similar being *M. philippinicus* Mapalo, Stec, Mirano-Bascos & Michalczyk, 2016 from the Philippines (KX129795, Mapalo *et al.* 2016), and the least similar being *M. dilimanensis* (MN257050, Itang *et al*. 2020).

Full matrices with *p*-distances are provided in Supplementary file 3.

Ecological notes

The location where the investigated moss sample was taken was characterized by the collector as a wet depression with a small temporary pond. But the genus *Lobohalacarus*, which was also found in the sample, is known to inhabit constant water bodies, primarily subterranean waters and areas where hypogean waters meet the surface (Bartsch 1995a), so the presence of this mite in the sample likely indicates that the type location for *Mesobiotus anastasiae* sp. nov. can be a permanently wet moss cushion. The presence of the single mite specimen can also be the result of an accidental introduction, but this seems to be less probable, because of the absence of permanent bodies of water in close proximity to the sampling site (I. Nikolaeva pers. com.) and the limited abilities of Halacaridae to tolerate desiccation.

Acknowledgements

I would like to thank Irina Nikolaeva (Zoological Institute, Russian Academy of Sciences, St. Petersburg) for collecting the material studied here. I thank Professor Giovanni Pilato and Professor Oscar Lisi (University of Catania, Italy) for giving me the opportunity to examine microscope slides of *Mesobiotus walteri* from Binda & Pilato's collection. I thank Professor Torbjørn Ekrem (Norwegian University of Science and Technology) for providing me with the unpublished DNA extraction protocol. I am grateful to Professor Łukasz Kaczmarek (Adam Mickiewicz University, Poznan, Poland) for permission to use his key for *Mesobiotus* species as a base for the key presented in this paper. I thank Peter Batson and Yuta Tamberg (University of Otago, Dunedin, New Zealand) for the linguistic review of the manuscript. This study was carried out with the use of equipment of the Core Facilities Centers: 'Culture Collection of Microorganisms', 'Centre for Molecular and Cell Technologies' and 'Centre for Microscopy and Microanalysis' of St. Petersburg State University.

References

Abe W. & Takeda M. 2000. Tardigrades from the Imperial Palace, Tokyo. *Memoirs of the National Science Museum Tokyo* 35: 165–177.

Abe W. & Takeda M. 2005. Semiterrestrial tardigrades from the Tokiwamatsu Imperial Villa, Tokyo, Japan. *Memoirs of the National Science Museum Tokyo* 39: 503–510.

Bartels P.J., Apodaca J.J., Mora C. & Nelson D.R. 2016. A global biodiversity estimate of a poorly known taxon: phylum Tardigrada. *Zoological Journal of the Linnean Society* 178 (4): 730–736. https://doi.org/10.1111/zoj.12441

Bartsch I. 1989. Süsswasserbewohnende Halacariden und ihre Einordnung in das System der Halacaroidea (Acari). *Acarologia* 30 (3): 217–239.

Bartsch I. 1995a. A new subspecies of the freshwater halacarid mite *Lobohalacarus weberi* (Romijn and Viets) (Halacaridae, Acari) from a Southern Atlantic Ocean island. *Annals of the Cape Provincial Museums, Natural History* 19: 171–180.

Bartsch I. 1995b. *Lobohalacarus subterraneus* n. sp., a freshwater halacarid (Acari: Halacaridae) from New Zealand. *New Zealand Journal of Zoology* 22: 209–212. https://doi.org/10.1080/03014223.1995.9518035

Bartsch I. 2008. Freshwater halacarid mites (Halacaridae: Prostigmata: Acari) from Tunesia, three new records and notes on geographical distribution of these species. *Entomologische Mitteilungen aus dem Zoologischen Museum Hamburg* 15 (178): 15–27.

Bartsch I. 2018. Freshwater halacarid mites (Acari: Halacaridae) from Madagascar – new records, keys and notes on distribution and biology. *Bonn zoological Bulletin* 67 (2): 79–99. https://doi.org/10.20363/BZB-2018.67.2.079

Beasley C.W. & Miller W.R. 2007. Tardigrada of Xinjiang Uygur Autonomous Region, China. *Journal of Limnology* 66 (S1): 49–55. https://doi.org/10.4081/jlimnol.2007.s1.49

Beasley C.W. & Miller W.R. 2012. Additional Tardigrada from Hubei Province, China, with the description of *Doryphoribius barbarae* sp. nov. (Eutardigrada: Parachela: Hypsibiidae). *Zootaxa* 3170 (1): 55–63. https://doi.org/10.11646/zootaxa.3170.1.5

Bertolani R., Guidetti R., Marchioro T., Altiero T., Rebecchi L. & Cesari M. 2014. Phylogeny of Eutardigrada: new molecular data and their morphological support lead to the identification of new evolutionary lineages. *Molecular Phylogenetics and Evolution* 76: 110–126. https://doi.org/10.1016/j.ympev.2014.03.006

Czechowski P., Sands C.J., Adams B.J., D'Haese C.A., Gibson J.A.E., McInnes S.J. & Stevens M.I. 2012. Antarctic Tardigrada: a first step in understanding molecular operational taxonomic units (MOTUs) and biogeography of cryptic meiofauna. *Invertebrate Systematics* 26: 526–538. https://doi.org/10.1071/IS12034

Dabert M., Witalinski W., Kazmierski A., Olszanowski Z. & Dabert J. 2010. Molecular phylogeny of acariform mites (Acari, Arachnida): strong conflict between phylogenetic signal and long-branch attraction artifacts. *Molecular Phylogenetics and Evolution* 56: 222–241. https://doi.org/10.1016/j.ympev.2009.12.020

Dastych H. & Harris J.M. 1995. A new species of the genus *Macrobiotus* from inland nunataks, Dronning Maud Land (Tardigrada). *Entomologische Mitteilungen aus dem Zoologischen Museum Hamburg* 11: 176–182.

Degma P., Bertolani R. & Guidetti R. (2009–2020). Actual checklist of Tardigrada species. 37th Edition: 03-07-2020. Available from https://doi.org/10.25431/11380_1178608 [accessed 24 Jul. 2020].

Edgar R.C. 2004. MUSCLE: multiple sequence alignment with high accuracy and high throughput. *Nucleic Acids Research* 32 (5): 1792–1797. https://doi.org/10.1093/nar/gkh340

Folmer O., Black M., Hoeh W., Lutz R. & Vrijenhoek R. 1994. DNA primers for amplification of mitochondrial cytochrome c oxidase subunit I from diverse metazoan invertebrates. *Molecular Marine Biology and Biotechnology* 3 (5): 294–299.

Gąsiorek P., Stec D., Zawierucha K., Kristensen R.M. & Michalczyk Ł. 2018. Revision of *Testechiniscus* Kristensen, 1987 (Heterotardigrada: Echiniscidae) refutes the polar-temperate distribution of the genus. *Zootaxa* 4472 (2): 261–297. https://doi.org/10.11646/zootaxa.4472.2.3

Gouy M., Guindon S. & Gascuel O. 2010. SeaView version 4: a multiplatform graphical user interface for sequence alignment and phylogenetic tree building. *Molecular Biology and Evolution* 27 (2): 221–224. https://doi.org/10.1093/molbev/msp259

Guidetti R., Gneuß E., Cesari M., Altiero T. & Schill R.O. 2019. Life-history traits and description of the new gonochoric amphimictic *Mesobiotus joenssoni* (Eutardigrada: Macrobiotidae) from the island of Elba, Italy. *Zoological Journal of the Linnean Society* 188: 848–859. https://doi.org/10.1093/zoolinnean/zlz077

Guil N., Jørgensen A. & Kristensen R. 2019. An upgraded comprehensive multilocus phylogeny of the Tardigrada tree of life. *Zoologica Scripta* 48 (1): 120–137. https://doi.org/10.1111/zsc.12321

Harvey M.S. 1988. A new species of *Lobohalacarus* from Australia (Chelicerata: Acarina: Halacaridae). *Memoirs of the Museum of Victoria* 49: 363–365. https://doi.org/10.24199/j.mmv.1988.49.15

Itang L.A.M., Stec D., Mapalo M.A., Mirano-Bascos D. & Michalczyk Ł. 2020. An integrative description of *Mesobiotus dilimanensis*, a new tardigrade species from the Philippines (Eutardigrada: Macrobiotidae: *furciger* group). *Raffles Bulletin of Zoology* 68: 19–31. https://doi.org/10.26107/RBZ-2020-0003

Kaczmarek Ł. & Michalczyk Ł. 2017. The *Macrobiotus hufelandi* group (Tardigrada) revisited. *Zootaxa* 4363 (1): 101–123. https://doi.org/10.11646/zootaxa.4363.1.4

Kaczmarek Ł., Cytan J., Zawierucha K., Diduszko D. & Michalczyk Ł. 2014. Tardigrades from Peru (South America), with descriptions of three new species of Parachela. *Zootaxa* 3790 (2): 357–379. https://doi.org/10.11646/zootaxa.3790.2.5

Kaczmarek Ł., Zawierucha K., Buda J., Stec D., Gawlak M., Michalczyk Ł. & Roszkowska M. 2018. An integrative redescription of the nominal taxon for the *Mesobiotus harmsworthi* group (Tardigrada: Macrobiotidae) leads to descriptions of two new *Mesobiotus* species from Arctic. *PLoS ONE* 13 (10): e0204756. https://doi.org/10.1371/journal.pone.0204756

Kaczmarek Ł., Bartylak T., Stec D., Kulpa A., Kepel M., Kepel A. & Roszkowska M. 2020. Revisiting the genus *Mesobiotus* Vecchi et al., 2016 (Eutardigrada, Macrobiotidae) – remarks, updated dichotomous key and an integrative description of new species from Madagascar. *Zoologischer Anzeiger* 287: 121–146. https://doi.org/10.1016/j.jcz.2020.05.003

Kumar S., Stecher G. & Tamura K. 2016. MEGA7: Molecular Evolutionary Genetics Analysis version 7.0 for bigger datasets. *Molecular Biology and Evolution* 33 (7): 1870–1874. https://doi.org/10.1093/molbev/msw054

Mapalo M., Stec D., Mirano-Bascos D.M. & Michalczyk Ł. 2016. *Mesobiotus philippinicus* sp. nov., the first limnoterrestrial tardigrade from the Philippines. *Zootaxa* 4126 (3): 411–426. https://doi.org/10.11646/zootaxa.4126.3.6

Mapalo M., Stec D., Mirano-Bascos D. & Michalczyk Ł. 2017. An integrative description of a limnoterrestrial tardigrade from the Philippines, *Mesobiotus insanis*, new species (Eutardigrada: Macrobiotidae: *harmsworthi* group). *Raffles Bulletin of Zoology* 65: 440–454.

Maucci W. & Durante Pasa M.V. 1980. Tardigradi muscicoli delle isole Andamane. *Bollettino del Museo Civico di Storia Naturale di Verona* 7: 281–291.

McInnes S.J., Michalczyk Ł. & Kaczmarek Ł. 2017. Annotated zoogeography of non-marine Tardigrada. Part IV: Africa. *Zootaxa* 4284 (1): 1–74. https://doi.org/10.11646/zootaxa.4284.1.1

Meyer H.A., Tsaliki M. & Hinton J.G. 2018. First records of water bears (Phylum Tardigrada) from Swaziland. *African Invertebrates* 59 (1): 47–53. https://doi.org/10.3897/AfrInvertebr.59.23191

Michalczyk Ł. & Kaczmarek Ł. 2003. A description of the new tardigrade *Macrobiotus reinhardti* (Eutardigrada: Macrobiotidae, *harmsworthi* group) with some remarks on the oral cavity armature within the genus *Macrobiotus* Schultze. *Zootaxa* 331 (1): 1–24. https://doi.org/10.11646/zootaxa.331.1.1

Michalczyk Ł. & Kaczmarek Ł. 2013. The Tardigrada Register: a comprehensive online data repository for tardigrade taxonomy. *Journal of Limnology* 72 (S1): e22. https://doi.org/10.4081/jlimnol.2013.s1.e22

Michalczyk Ł., Wełnicz W., Frohme M. & Kaczmarek Ł. 2012. Redescriptions of three *Milnesium* Doyère, 1840 taxa (Tardigrada: Eutardigrada: Milnesiidae), including the nominal species for the genus. *Zootaxa* 3154 (1): 1–20. https://doi.org/10.11646/zootaxa.3154.1.1

Middleton R.C. 2003. Tardigrades in southern Africa. *African Journal of Ecology* 41: 280–282. https://doi.org/10.1046/j.1365-2028.2003.00439.x

Mironov S.V., Dabert J. & Dabert M. 2012. A new feather mite species of the genus *Proctophyllodes* Robin, 1877 (Astigmata: Proctophyllodidae) from the Long-tailed Tit *Aegithalos caudatus* (Passeriformes: Aegithalidae) – morphological description with DNA barcode data. *Zootaxa* 3253 (1): 54–61. https://doi.org/10.11646/zootaxa.3253.1.2

Pilato G. 1974. Tre nouve specie di Tardigradi muscicoli di Cina. *Animalia* 1: 59–68.

Pilato G. 1981. Analisi di nuovi caratteri nello studio degli Eutardigradi. *Animalia* 8 (1/3): 51–57.

Pilato G. & Binda M.G. 2010. Definition of families, subfamilies, genera and subgenera of the Eutardigrada, and keys to their identification. *Zootaxa* 2404 (1): 1–54. https://doi.org/10.11646/zootaxa.2404.1.1

Pleijel F., Jondelius U., Norlinder E., Nygren A., Oxelman B., Schander C., Sundberg P. & Thollesson M. 2008. Phylogenies without roots? A plea for the use of vouchers in molecular phylogenetic studies. *Molecular Phylogenetics and Evolution* 48 (1): 369–371. https://doi.org/10.1016/j.ympev.2008.03.024

Rossi G., Claps M. & Ardohain D. 2009. Tardigrades from northwestern Patagonia (Neuquén Province, Argentina) with the description of three new species. *Zootaxa* 2095 (1): 21–36. https://doi.org/10.11646/zootaxa.2095.1.3

Roszkowska M., Stec D., Gawlak M. & Kaczmarek Ł. 2018. An integrative description of a new tardigrade species *Mesobiotus romani* sp. nov (Macrobiotidae; *harmsworthi* group) from the Ecuadorian Pacific coast. *Zootaxa* 4450 (5): 550–564. https://doi.org/10.11646/zootaxa.4450.5.2

Sands C.J., McInnes S.J., Marley N.J., Goodall-Copestake W., Convey P. & Linse K. 2008. Phylum Tardigarda: an "individual" approach. *Cladistics* 24: 1–18. https://doi.org/10.1111/j.1096-0031.2008.00219.x

Stec D. 2019. *Mesobiotus datanlanicus* sp. nov., a new tardigrade species (Macrobiotidae: *Mesobiotus harmsworthi* group) from Lâm Đồng Province in Vietnam. *Zootaxa* 4679 (1): 164–180. https://doi.org/10.11646/zootaxa.4679.1.10

Stec D. & Kristensen R.M. 2017. An integrative description of *Mesobiotus ethiopicus* sp. nov. (Tardigrada: Eutardigrada: Parachela: Macrobiotidae: *harmsworthi* group) from the northern Afrotropic region. *Turkish Journal of Zoology* 41: 800–811. https://doi.org/10.3906/zoo-1701-47

Stec D., Smolak R., Kaczmarek Ł. & Michalczyk Ł. 2015. An integrative description of *Macrobiotus paulinae* sp. nov. (Tardigrada: Eutardigrada: Macrobiotidae: *hufelandi* group) from Kenya. *Zootaxa* 4052 (5): 501–526. https://doi.org/10.11646/zootaxa.4052.5.1

Stec D., Gąsiorek P., Morek W., Kosztyła P., Zawierucha K., Michno K., Kaczmarek Ł., Prokop Z.M. & Michalczyk Ł. 2016. Estimating optimal sample size for tardigrade morphometry. *Zoological Journal of the Linnean Society* 178 (4): 776–784. https://doi.org/10.1111/zoj.12404

Stec D., Zawierucha K. & Michalczyk Ł. 2017. An integrative description of *Ramazzottius subanomalus* (Biserov, 1985) (Tardigrada) from Poland. *Zootaxa* 4300 (3): 403–420. https://doi.org/10.11646/zootaxa.4300.3.4

Stec D., Morek W., Gąsiorek P. & Michalczyk Ł. 2018a. Unmasking hidden species diversity within the *Ramazzottius oberhaeuseri* complex, with an integrative redescription of the nominal species for the family Ramazzottiidae (Tardigrada: Eutardigrada: Parachela). *Systematics and Biodiversity* 16 (4): 357–376. https://doi.org/10.1080/14772000.2018.1424267

Stec D., Roszkowska M., Kaczmarek Ł. & Michalczyk Ł. 2018b. An integrative description of a population of *Mesobiotus radiatus* (Pilato, Binda & Catanzaro, 1991) from Kenya. *Turkish Journal of Zoology* 42: 523–540. https://doi.org/10.3906/zoo-1802-43

Stec D., Kristensen R.M. & Michalczyk Ł. 2020. An integrative description of *Minibiotus ioculator* sp. nov. from the Republic of South Africa with notes on *Minibiotus pentannulatus* Londoño et al., 2017 (Tardigrada: Macrobiotidae). *Zoologischer Anzeiger* 286: 117–134. https://doi.org/10.1016/j.jcz.2020.03.007

Tumanov D.V. 2018a. *Hypsibius vaskelae*, a new species of Tardigrada (Eutardigrada, Hypsibiidae) from Russia. *Zootaxa* 4399 (3): 434–442. https://doi.org/10.11646/zootaxa.4399.3.12

Tumanov D.V. 2018b. *Mesobiotus nikolaevae* sp. n. (Eutardigrada: Macrobiotidae), a new species of Tardigrada from Croatia. *Invertebrate Zoology* 15 (4): 402–419. https://doi.org/10.15298/invertzool.15.4.08

Tumanov D.V. & Pilato G. 2019. A new species of Eutardigrade (Macrobiotidae) from New Zealand. *Zootaxa* 4603 (3): 537–548. https://doi.org/10.11646/zootaxa.4603.3.6

Utsugi K. 1988. Tardigrades in Hokkaido area. *Zoological Science* 5 (4): 1335.

Vecchi M., Cesari M., Bertolani R., Jönsson K.I., Rebecchi L. & Guidetti R. 2016. Integrative systematic studies on tardigrades from Antarctica identify new genera and new species within Macrobiotoidea and Echiniscoidea. *Invertebrate Systematics* 30 (4): 303–322. https://doi.org/10.1071/IS15033

Manuscript received: 28 August 2020
Manuscript accepted: 24 September 2020
Published on: 4 December 2020
Topic editor: Rudy Jocqué
Section editor: Daniel Piotr Stec
Desk editor: Pepe Fernández

Printed versions of all papers are also deposited in the libraries of the institutes that are members of the *EJT* consortium: Muséum national d'histoire naturelle, Paris, France; Meise Botanic Garden, Belgium; Royal Museum for Central Africa, Tervuren, Belgium; Royal Belgian Institute of Natural Sciences, Brussels, Belgium; Natural History Museum of Denmark, Copenhagen, Denmark; Naturalis Biodiversity Center, Leiden, the Netherlands; Museo Nacional de Ciencias Naturales-CSIC, Madrid, Spain; Real Jardín Botánico de Madrid CSIC, Spain; Zoological Research Museum Alexander Koenig, Bonn, Germany; National Museum, Prague, Czech Republic.

Supplementary material

Supplementary file 1. DNA extraction protocol. https://doi.org/10.5852/ejt.2020.726.1179.3271

Supplementary file 2. Raw morphometric data for *Mesobiotus anastasiae* sp. nov. https://doi.org/10.5852/ejt.2020.726.1179.3273

Supplementary file 3. Matrices of *p*-distances for species of *Mesobiotus* Vecchi, Cesari, Bertolani, Jönsson & Guidetti, 2016. https://doi.org/10.5852/ejt.2020.726.1179.3275

Appendix 1 (continued on next page). Complete list of sequences used for molecular comparisons between the new *Mesobiotus* species described in this study and all other species of the genus *Mesobiotus* for which homologous DNA sequences are currently available.

Gene	Species	Accession number	Source
COI	***Mesobiotus anastasiae* sp. nov.**	**MT904513**	**this study**
	Mesobiotus cf. *barabanovi* (Tumanov, 2005)	MN313170	Kaczmarek *et al*. 2020
	Mesobiotus datanlanicus Stec, 2019	MK578905	Stec 2019
	Mesobiotus dilimanensis Itang *et al*., 2020	MN257047	Itang *et al*. 2020
	Mesobiotus ethiopicus Stec & Kristensen, 2017	MF678794	Stec & Kristensen 2017
	Mesobiotus fiedleri Kaczmarek *et al*., 2020	MH676056	Kaczmarek *et al*. 2020
	Mesobiotus furciger (Murray, 1907)	JX865306, JX865308, JX865314,	Czechowski *et al*. 2012
	Mesobiotus harmsworthi (Murray, 1907)	MH195150, MH195151	Kaczmarek *et al*. 2018
	Mesobiotus hilariae Vecchi *et al*., 2016	KT226108	Vecchi *et al*. 2016
	Mesobiotus insanis Mapalo *et al*., 2017	MF441491	Mapalo *et al*. 2017
	Mesobiotus occultatus Kaczmarek *et al*., 2018	MH195152	Kaczmarek *et al*. 2018
	Mesobiotus philippinicus Mapalo *et al*., 2016	KX129796	Mapalo *et al.* 2016
	Mesobiotus radiatus (Pilato *et al*., 1991)	MH195148	Stec *et al*. 2018b
	Mesobiotus romani Roszkowska *et al*., 2018	MH195149	Roszkowska *et al*. 2018
	Mesobiotus gr. *furciger*	MH195153	Kaczmarek *et al*. 2018
	Mesobiotus gr. *harmsworthi*	MH195154	Kaczmarek *et al*. 2018
18S rRNA	***Mesobiotus anastasiae* sp. nov.**	**MT903468**	**this study**
	Mesobiotus cf. *barabanovi* (Tumanov, 2005)	MN310392	Kaczmarek *et al*. 2020
	Mesobiotus datanlanicus Stec, 2019	MK584659	Stec 2019
	Mesobiotus dilimanensis Itang *et al*., 2020	MN257048	Itang *et al*. 2020
	Mesobiotus ethiopicus Stec & Kristensen, 2017	MF678793	Stec & Kristensen 2017
	Mesobiotus fiedleri Kaczmarek *et al*., 2020	MH681585	Kaczmarek *et al*. 2020
	Mesobiotus furciger (Murray, 1907)	EU266927, EU266928, EU266929	Sands *et al.* 2008
	Mesobiotus harmsworthi (Murray, 1907)	MH197146	Kaczmarek *et al*. 2018
	Mesobiotus hilariae Vecchi *et al*., 2016	KT226068, KT226069, KT226070, KT226071	Vecchi *et al*. 2016
	Mesobiotus insanis Mapalo *et al*., 2017	MF441488	Mapalo *et al*. 2017
	Mesobiotus cf. *mottai* (Binda & Pilato, 1994)	KT226072	Vecchi *et al*. 2016
	Mesobiotus occultatus Kaczmarek *et al*., 2018	MH197147	Kaczmarek *et al*. 2018
	Mesobiotus philippinicus Mapalo *et al*., 2016	KX129793	Mapalo *et al.* 2016
	Mesobiotus polaris (Murray, 1910)	KT226075, KT226076, KT226077, KT226078	Vecchi *et al*. 2016
	Mesobiotus radiatus (Pilato *et al*., 1991)	MH197153	Stec *et al*. 2018b

Appendix 1 (continued)**.**

Gene	Species	Accession number	Source
	Mesobiotus romani Roszkowska *et al*., 2018	MH197158	Roszkowska *et al*. 2018
	Mesobiotus gr. *furciger*	MH197148	Kaczmarek *et al*. 2018
	Mesobiotus gr. *harmsworthi*	MH197149	Kaczmarek *et al*. 2018
	Mesobiotus gr. *harmsworthi*	KT226073, KT226074	Vecchi *et al*. 2016
	Mesobiotus gr. *harmsworthi*	HQ604967, HQ604968, HQ604969, HQ604970	Bertolani *et al.* 2014
28S rRNA	***Mesobiotus anastasiae* sp. nov.**	**MT903612**	**this study**
	Mesobiotus cf. *barabanovi* (Tumanov, 2005)	MN310388	Kaczmarek *et al*. 2020
	Mesobiotus datanlanicus Stec, 2019	MK584658	Stec 2019
	Mesobiotus dilimanensis Itang *et al*., 2020	MN257049	Itang *et al*. 2020
	Mesobiotus ethiopicus Stec & Kristensen, 2017	MF678792	Stec & Kristensen 2017
	Mesobiotus fiedleri Kaczmarek *et al*., 2020	MH681693	Kaczmarek *et al*. 2020
	Mesobiotus harmsworthi (Murray, 1907)	MH197264	Kaczmarek *et al*. 2018
	Mesobiotus insanis Mapalo *et al*., 2017	MF441489	Mapalo *et al*. 2017
	Mesobiotus philippinicus Mapalo *et al*., 2016	KX129794	Mapalo *et al.* 2016
	Mesobiotus radiatus (Pilato *et al*., 1991)	MH197152	Stec *et al*. 2018b
	Mesobiotus romani Roszkowska *et al*., 2018	MH197151	Roszkowska *et al*. 2018
	Mesobiotus gr. *furciger*	MH197265	Kaczmarek *et al*. 2018
	Mesobiotus gr. *harmsworthi*.	MH197266	Kaczmarek *et al*. 2018
ITS-2	***Mesobiotus anastasiae* sp. nov.**	**MT903470**	**this study**
	Mesobiotus cf. *barabanovi*	MN310390	Kaczmarek *et al*. 2020
	Mesobiotus datanlanicus Stec, 2019	MK584657	Stec 2019
	Mesobiotus dilimanensis Itang *et al*., 2020	MN257050	Itang *et al*. 2020
	Mesobiotus ethiopicus Stec & Kristensen, 2017	MN122776	Stec & Kristensen 2017
	Mesobiotus fiedleri Kaczmarek *et al*., 2020	MH681724	Kaczmarek *et al*. 2020
	Mesobiotus harmsworthi (Murray, 1907)	MH197154	Kaczmarek *et al*. 2018
	Mesobiotus insanis Mapalo *et al*., 2017	MF441490	Mapalo *et al*. 2017
	Mesobiotus occultatus Kaczmarek *et al*., 2018	MH197155	Kaczmarek *et al*. 2018
	Mesobiotus philippinicus Mapalo *et al*., 2016	KX129795	Mapalo *et al.* 2016
	Mesobiotus radiatus (Pilato *et al*., 1991)	MH197267, MH197268	Stec *et al*. 2018b
	Mesobiotus romani Roszkowska *et al*., 2018	MH197150	Roszkowska *et al*. 2018
	Mesobiotus gr. *furciger*	MH197156	Kaczmarek *et al*. 2018
	Mesobiotus gr. *harmsworthi*	MH197157	Kaczmarek *et al*. 2018

Appendix 2. Key to the species of the genus *Mesobiotus* Vecchi, Cesari, Bertolani, Jönsson & Guidetti, 2016.

A key to the *Mesobiotus* species was published recently (Kaczmarek *et al.* 2020). Unfortunately, two species (*M. nikolaevae* Tumanov, 2018 and *M. helenae* Tumanov & Pilato, 2019) were not included in this work, and three additional species (*M. datanlanicus* Stec, 2019, *M. dilimanensis* Itang, Stec, Mapalo, Mirano-Bascos & Michalczyk, 2020 and *M. joenssoni* Guidetti, Gneuß, Cesari, Altiero & Schill, 2019) are not present because the key predates their descriptions. Further, some minor inaccuracies in the key were revealed. Here I present an updated key to the species of the genus *Mesobiotus*, including all above-mentioned omitted species, as well as the new species described here. The key is based on the version published by Kaczmarek *et al.* (2020). *Mesobiotus meridionalis* (Richters, 1909) nom. inq., *M. polaris* (Murray, 1910) nom. inq., *M. stellaris* (du Bois-Reymond Marcus, 1944) nom. inq. and *M. armatus* (Pilato & Binda, 1996) nom. inq. were excluded from the key, following Kaczmarek *et al.* (2020).

1. Dorsal cuticle with sculptured surface (visible in PhC as granulation or thin reticulate pattern) or with pores or stripes of pigmentation 2
– Cuticle smooth (except for minute regular granulation visible only in SEM) 11

2. Stripes of pigmentation present ..... ***M. baltatus*** (McInnes, 1991)
– Stripes of pigmentation absent 3

3. First band in oral cavity present 4
– First band in oral cavity absent or not visible in PCM ..... ***M. perfidus*** (Pilato & Lisi, 2009)

4. Cuticle with pores without granulation on the body surface or on legs, oral cavity armature without longitudinally elongated teeth in the second band, egg processes in shape of cones with long slender endings, egg processes with "bubbles", egg processes bases without crown of thickenings .... ***M. krynauwi*** (Dastych & Harris, 1995)
– Cuticle with sculpture, visible in PhC as granulation or dot-like sculpture, or with thin reticulate pattern, without pores 5

5. Cuticular sculpture consists of relatively large granules, well-visible in PhC (granules size ≥ 1 μm) in the caudal region of the dorsal body surface 6
– Cuticular sculpture without large granules, with fine dot-like sculpture poorly visible in LM or with thin reticulate pattern only 7

6. Granules of the cuticular sculpture are present from the level of the third legs to the posterior end of the animal, *pt* of stylet supports 72.41–83.64, egg processes 27–36 μm high, with collar and large pores above it .....***M. joenssoni*** Guidetti, Gneuß, Cesari, Altiero & Schill, 2019
– Granules of the cuticular sculpture are present only on the caudal extremity of the body, *pt* of stylet supports ca 85.4, maximal height of egg processes is 19 μm ....***M. arguei*** (Pilato & Sperlinga, 1975)

7. Cuticular sculpture appears in PhC as thin reticulate pattern, oral cavity armature without longitudinally elongated teeth in the second band, with one row of elongated teeth in the first band, egg processes with collar and large pores above it ..... ***M. anastasiae*** sp. nov.
– Cuticular sculpture consists of fine granules or tubercles, poorly visible in PhC, without reticular pattern, oral cavity armature with longitudinally elongated teeth in the second band 8

8. Egg shell porous ..... ***M. sicheli*** (Binda, Pilato & Lisi, 2005)
– Egg shell different 9

9. Egg shell surface with reticular sculpture, egg processes smooth, number of egg processes on the circumference 22 or more, width of egg processes bases less than 8.9 µm ..... ***M. contii*** (Pilato & Lisi, 2006)
– Egg shell surface smooth, egg processes with reticular design, number of egg processes on the circumference 21 or less, width of egg processes bases 8.9 µm or more 10

10. Lunules under claws IV smooth, eyes absent, the egg processes bases elongated into long stripes which forms the areolation (5–7 areoles around each egg process) on the egg shell surface (full areolation) ..... ***M. pseudonuragicus*** (Pilato, Binda & Lisi, 2004)
– Lunules under claws IV with indented margin, eyes present, areolation on the egg surface absent, egg process bases with crown of thickenings ..... ***M. pseudocoronatus*** (Pilato, Binda & Lisi, 2006)

11. The egg processes in shape of flat hemispherical domes 12
– The egg processes in shape of cones or "mammillate-like domes" 13

12. The egg surface with reticular sculpture, egg processes bases without crown of thickenings ..... ***M. montanus*** (Murray, 1910)
– The egg surface without reticular sculpture, egg processes bases with crown of thickenings and wrinkles ..... ***M. mottai*** (Binda & Pilato, 1994)

13. The egg processes "mammillate-like domes" 14
– The egg processes in shape of cones 15

14. The egg processes bases with finger-like projections, egg processes with reticular design and without additional, small hemispherical projections on the top, number of egg processes on the circumference 16 or more, width of egg processes bases more than 11.0 µm ..... ***M. peterseni*** (Maucci, 1991)
– The egg processes bases with finger-like projections, egg processes without reticular design and with additional, small hemispherical projections on the top, number of egg processes on the circumference 15 or less, width of egg processes bases less than 7.0 µm ..... ***M. lusitanicus*** (Maucci & Durante Pasa, 1984)

15. Egg processes with basal collar, egg shell with polygonal relief ..... ***M. mauccii*** (Pilato, 1974)
– Egg processes without collar, egg shell without polygonal relief 16

16. The egg processes in shape of truncated cones ..... ***M. zhejiangensis*** (Yin, Wang & Li, 2011)
– The egg processes different 17

17. The egg processes bases elongated into long stripes that form the areolation on the egg shell surface (full areolation) 18
– Full areolation on egg shell surface absent 26

18. First band of teeth in oral cavity absent 19
– First band of teeth in oral cavity present 20

19. Lunules under claws IV smooth, egg processes in shape of cones with long slender endings ..... ***M. ovostriatus*** (Pilato & Patanè, 1998)
– Lunules under claws IV indented, egg processes in shape of sharp wide cones ..... ***M. hilariae*** Vecchi, Cesari, Bertolani, Jøonsson, Rebecchi & Guidetti, 2016

20. Egg processes with terminal filaments 21
– Egg processes without terminal filaments 22

21. Eyes absent, macroplacoid length sequence (2 < 1 < 3), process apices divided into at least 15 filaments ..... ***M. insanis*** Mapalo, Stec, Mirano-Bascos & Michalczyk, 2017
– Eyes present, macroplacoid length sequence (2 < 1 = 3), process apices divided into 2–5 filaments ..... ***M. nuragicus*** (Pilato & Sperlinga, 1975)

22. Egg processes are usually terminated by a multifurcated crown of several finger-shaped appendages, which often are terminated by short spines ..... ***M. datanlanicus*** Stec, 2019
– Egg processes without crown of appendages at the top 23

23. Egg processes in shape of cones with long slender endings ..... ***M. barbarae*** (Kaczmarek, Michalczyk & Degma, 2007)
– Egg processes sharp, narrow or wide cones 24

24. Granulation on legs absent, egg processes in the shape of sharp wide cones, height of egg processes less than 16.0 µm ..... ***M. neuquensis*** (Rossi, Claps & Ardohain, 2009)
– Granulation on legs present, egg processes in the shape of sharp narrow cones, height of egg processes more than 24.0 µm 25

25. The *pt* of stylet supports less than 75.0, six areoles around each egg process, height of egg processes less than 35.0 µm, width of egg processes bases less than 22.0 µm ..... ***M. hieronimi*** (Pilato & Claxton, 1988)
– The *pt* of stylet supports more than 77.0, sixteen areoles around each egg process, height of egg processes more than 41.0 µm, width of egg processes bases more than 27.0 µm ..... ***M. pseudoliviae*** (Pilato & Binda, 1996)

26. Egg processes bases elongated into long stripes, which form the semi-areolation (the branches at least in some cases not connected to each other) 27
– Egg processes bases different 31

27. Eyes absent, egg processes with filaments ..... ***M. ethiopicus*** Stec & Kristensen, 2017
– Eyes present, egg processes without filaments 28

28. Additional teeth in oral cavity armature present, egg processes with “bubbles” 29
– Additional teeth in oral cavity armature absent, egg processes without “bubbles” 30

29. Claws IV with large, protruding accessory points, egg processes with reticular design, number of egg processes on the circumference 11–12 ..... ***M. harmsworthi*** (Murray, 1907)
– Large and protruding accessory points on claws IV absent, egg processes without reticular design, number of egg processes on the circumference 15–24 ..... ***M. blocki*** (Dastych, 1984)

30. Granulation on legs I–III absent, egg processes in shape of cones with long slender endings, number of egg processes on the circumference ca 20 ..... ***M. barabanovi*** (Tumanov, 2005)
– Granulation on legs I–III present, egg processes in shape of sharp wide cones, number of egg processes on the circumference 10–12 ..... ***M. skoracki*** Kaczmarek, Zawierucha, Buda, Stec, Gawlak, Michalczyk & Roszkowska, 2018

31. Egg processes with finger-like projections, i.e., egg processes bases elongated into long stripes, but never connected to each other 32
– Egg processes without finger-like projections 39

32. Egg processes in shape of cones with long slender endings 33

– Egg processes in the shape of sharp, narrow or wide cones 35

33. Egg processes with "bubbles" and flexible filaments in apical part, height of egg processes less than 13.0 µm ..... ***M. pseudoblocki*** Roszkowska, Stec, Ciobanu & Kaczmarek, 2016
– Egg processes without "bubbles" or flexible filaments in apical part, height of egg processes more than 20.0 µm 34

34. Eyes present, number of egg processes on the circumference 6–8, height of egg processes 50.0 µm or more ..... ***M. liviae*** (Ramazzotti, 1962)
– Eyes absent, number of egg processes on the circumference ca 12, height of egg processes ca 21.0 µm ..... ***M. snaresensis*** (Horning, Schuster & Grigarick, 1978)

35. Egg processes with "bubbles", in shape of sharp narrow cones 36
– Egg processes without "bubbles", in shape of sharp wide cones 38

36. Eyes absent, additional teeth in oral cavity absent ..... ***M. tehuelchensis*** (Rossi, Claps & Ardohain, 2009)
– Eyes present, additional teeth in oral cavity present 37

37. Finger-like projections very small, present only on some processes and irregularly distributed ..... ***M. reinhardti*** (Michalczyk & Kaczmarek, 2003)
– Six, large and regularly distributed finger-like projections present on all processes ..... ***M. szeptyckii*** (Kaczmarek & Michalczyk, 2009)

38. Eyes and first band of teeth in oral cavity present, *pt* of stylet supports 77.0 or more, egg full diameter (with processes) 100.0–116.0 µm, number of egg processes on the circumference 8–9, height of egg processes 12.0–24.0 µm ..... ***M. erminiae*** (Binda & Pilato, 1999)
– Eyes absent, first band of teeth in oral cavity absent or not visible in PCM, *pt* of stylet supports 75.5 or less, egg full diameter (with processes) 88.0–92.0 µm, number of egg processes on the circumference 12–15, height of egg processes 9.0–11.0 µm ..... ***M. diguensis*** (Pilato & Lisi, 2009)

39. Egg processes with reticular design 40
– Egg processes smooth or with refracting areas 56

40. First band of teeth in oral cavity absent or not visible in PCM 41
– First band of teeth in oral cavity present 42

41. Eyes present, lunules under claws IV indented, granulation on legs I–III present, number of egg processes on the circumference 15–17 ..... ***M. philippinicus*** Mapalo, Stec, Mirano-Bascos & Michalczyk, 2016
– Eyes absent, lunules under claws IV smooth, granulation on legs I–III absent, number of egg processes on the circumference 11–12 ..... ***M. pseudopatiens*** Kaczmarek & Roszkowska, 2016

42. Egg processes with terminal filaments (at least a significant part of them) 43
– Egg processes without terminal filaments 48

43. Egg processes in the shape of sharp wide cones 44
– Egg processes in the shape of cones with long, slender endings 45

44. Egg processes with bunch of short filaments, number of egg processes on the circumference 10–12, width of egg processes bases 14.5–22.5 µm ..... ***M. radiatus*** (Pilato, Binda & Catanzaro, 1991)

– Egg processes with few long filaments, number of egg processes on the circumference 15–17, width of egg processes bases 10.0–14.0 μm ..... ***M. dimentmani*** (Pilato, Lisi & Binda, 2010)

45. Lunules under claws IV without indentation ..... ***M. nikolaevae*** Tumanov, 2018
– Lunules under claws IV indented 46

46. Egg processes bases without distinct crown of thickenings, processes are connected with very thin ridges ..... ***M. diffusus*** (Binda & Pilato, 1987)
– Egg processes bases with distinct crown of thickenings, egg surface between processes with dots and wrinkles 47

47. Eyes present, lunules under claws IV with 4–5 denticles, egg processes tips sometimes trifurcated ..... ***M. wuzhishanensis*** (Yin, Wang & Li, 2011)
– Eyes absent, lunules under claws IV with more than 5 denticles, egg processes tips never trifurcated ..... ***M. romani*** Roszkowska, Stec, Gawlak & Kaczmarek, 2018

48. Egg processes in the shape of sharp wide cones 49
– Egg processes in the shape of cones with long, slender endings 53

49. Lunules under claws IV indented ..... ***M. simulans*** (Pilato, Binda, Napolitano & Moncada, 2000)
– Lunules under claws IV smooth 50

50. Additional teeth in oral cavity present, egg bare diameter (without processes) 55.0 or less, egg full diameter (with processes) 71.0 μm or less, width of egg processes bases less than 10.5 ..... ***M. coronatus*** (De Barros, 1942)
– Additional teeth in oral cavity absent, egg bare diameter (without processes) 59.0 or more, egg full diameter (with processes) 73.0 μm or more, width of egg processes bases 11.1 or more 51

51. The basal tract of posterior and anterior claws IV much longer, primary and secondary branches forming an almost 90° angle (Pilato *et al*., 2014: fig. 1d) ..... ***M. insuetus*** (Pilato, Sabella & Lisi, 2014)
– Typical *Mesobiotus* claws IV 52

52. Eyes absent, macroplacoid length sequence (2 < 3 < 1), additional teeth in oral cavity absent, height of egg processes 8–16 μm ..... ***M. patiens*** (Pilato, Binda, Napolitano & Moncada, 2000)
– Eyes present, macroplacoid length sequence (2 < 3 ≤ 1), with additional teeth in the ventral portion of the oral cavity, height of egg processes 14.1–21.8 μm ..... ***M. occultatus*** Kaczmarek, Zawierucha, Buda, Stec, Gawlak, Michalczyk & Roszkowska, 2018

53. Egg shell porous, egg processes bases without crown of thickenings, height of egg processes 22.0 μm or more, width of egg processes 17.0 μm or more ..... ***M. altitudinalis*** (Biserov, 1997–98)
– Egg shell smooth or with dots and/or wrinkles, egg processes bases with crown of thickenings, height of egg processes 16.5 μm or less, width of egg processes 15.5 μm or less 54

54. Egg processes consists of wide short conical basal part very distinctly separated from the apical part in form of a thin long spine with poorly visible internal structure, number of egg processes on the circumference 27–32 ..... ***M. binieki*** (Kaczmarek, Gołdyn, Prokop & Michalczyk, 2011)
– Egg processes with less abruptly separated basal and apical parts, apical part with well visible internal "bubbles", number of egg processes on the circumference less than 23 55

55. Number of egg processes on the circumference ca 12, height of egg processes 15.2–16.2 µm, with well visible reticular design of the egg processes, apical parts of egg processes rigid and never subdivided, egg surface with radial ridges ..... ***M. rigidus*** (Pilato & Lisi, 2006)
– Number of egg processes on the circumference ca 22, height of egg processes 11.0 µm, with faint and almost invisible reticular design of the egg processes, apical parts of egg processes flexible and rarely bifurcated, egg surface smooth ..... ***M. helenae*** Tumanov & Pilato, 2019

56. The egg processes in the shape of rough cones, egg processes bases smooth .... ***M. kovalevi*** (Tumanov, 2004)
– The egg processes in the shape of branched or sharp wide cones, egg processes bases with crown of thickenings or wrinkles 57

57. The egg processes in the shape of sharp wide cones, the egg shell surface without pores or reticular sculpture ..... ***M. australis*** (Pilato & D'Urso, 1976)
– The egg processes in the shape of branched cones, the egg shell surface porous or with reticular sculpture 58

58. The egg processes with refracting areas 59
– The egg processes without refracting areas 61

59. Bases of egg processes without band of pores, large and numerous refracting areas visible on the apical part of all processes ..... ***M. furciger*** (Murray, 1907)
– Bases of egg processes with band of pores, small and single refracting areas present only on some processes 60

60. Apical parts of egg processes always divided into 2–4 branches, height of egg processes ca 15.0 µm, *pt* of buccal tube width 22.8–25.4 ..... ***M. pilatoi*** (Binda & Rebecchi, 1992)
– At least some of apical part of egg processes not divided, height of egg processes 8.5–13.1 µm, *pt* of buccal tube width 16.5–18.6 .... ***M. fiedleri*** Kaczmarek, Bartylak, Stec, Kulpa, M. Kepel, A. Kepel & Roszkowska, 2020

61. The egg shell surface with reticular sculpture or ridges, without pores 62
– The egg shell surface porous 65

62. The egg processes in the shape of branched cones with long slender endings, the egg shell surface with ridges radiating from process bases, only sometimes resembling reticulate pattern, height of egg processes 10.7–11.8 µm, width of egg processes 7.4–10.0 µm .... ***M. siamensis*** (Tumanov, 2006)
– The egg processes in the shape of branched cones, the egg shell surface with clearly reticular sculpture, height of egg processes less than 10.0 µm, width of egg processes usually less than 7.0 µm (up to 7.5 in *M. dilimanensis*) 63

63. The *pt* of stylet supports less than 76.5, egg processes sparsely distributed over the egg surface, number of egg processes on the circumference ca 17, egg processes with relatively long branches, nearly equal in length to the basal part, with multiple bifurcations, height of egg processes 4.7–4.8 µm ..... ***M. divergens*** (Binda, Pilato & Lisi, 2005)
– The *pt* of stylet supports more than 77.0, egg processes densely distributed over the egg surface, egg processes with relatively short branches, distinctly shorter than the basal part, height of egg processes usually exceeds 4.8 µm 64

64. Additional teeth in oral cavity absent, granulation on legs I–III present, *pt* of the buccal tube external width 14.0–17.4, number of egg processes on the circumference 18–24 .... ***M. dilimanensis*** Itang, Stec, Mapalo, Mirano-Bascos & Michalczyk, 2020
– Additional teeth in oral cavity present, granulation on legs I–III absent, *pt* of the buccal tube external width 17.9–19.6, number of egg processes on the circumference 27–30 .... ***M. creber*** (Pilato & Lisi, 2009)

65. Egg processes divided close to or at the top, number of egg processes on the circumference ca 25, width of egg processes 7.3–7.8 µm ..... ***M. orcadensis*** (Murray, 1907)
– Egg processes begin to divide in the middle of their length, number of egg processes on the circumference 21–23, width of egg processes 8.4–9.5 µm .... ***M. aradasi*** (Binda, Pilato & Lisi, 2005)